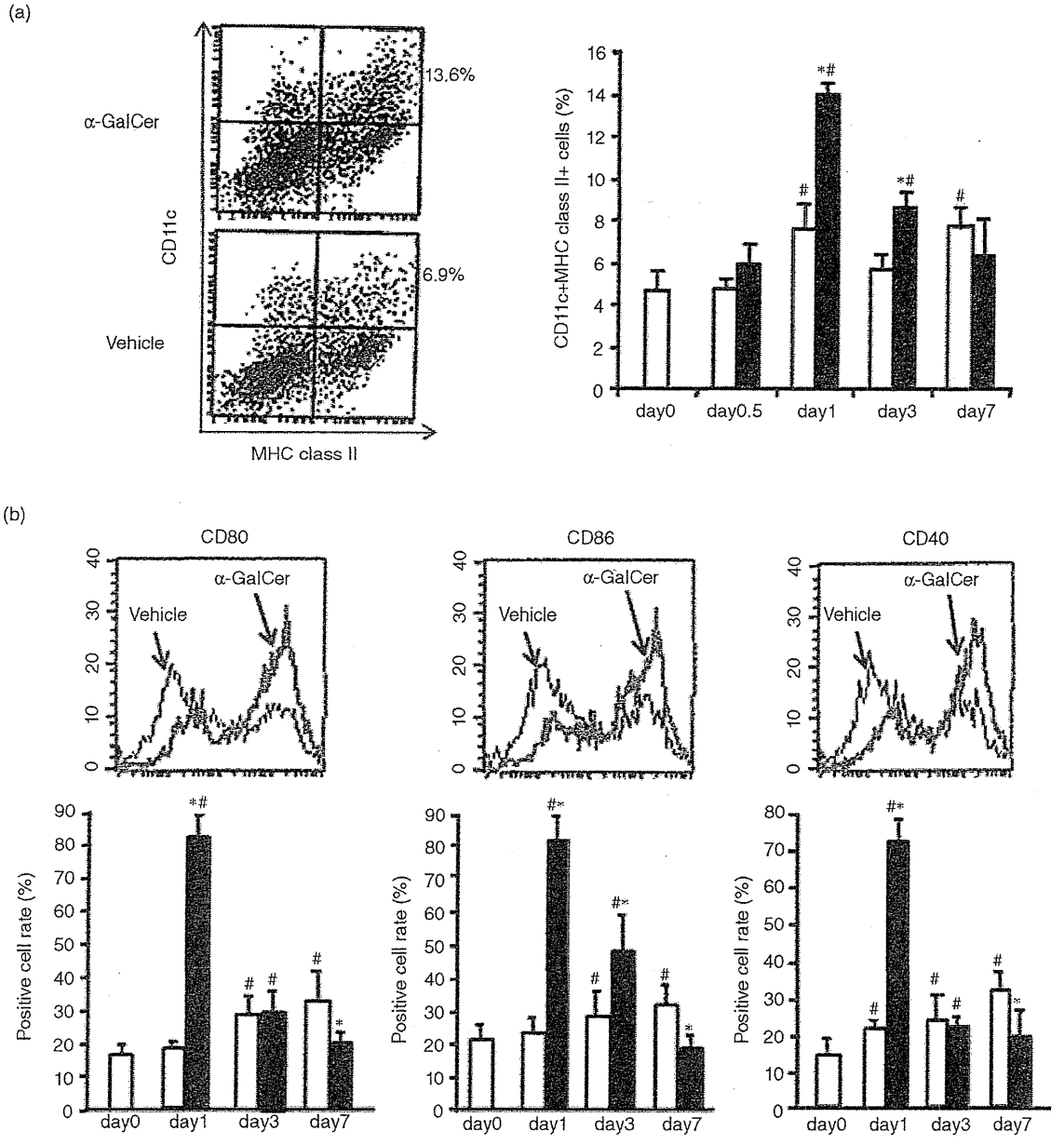

Figure 2 α-Galactosylceramide (α-GalCer) treatment increased dendritic cell (DC) population in the liver mononuclear cells (MNC) and activated DC functions. (a) BALB/c mice were treated with α-GalCer or vehicle. Hepatic MNC were prepared on days 0, 0.5, 1, 3 and 7. DC ($CD11c^+$ major histocompatibility complex [MHC] class II^+ cells) population was evaluated by flow cytometry. White bar, vehicle-treated mice; black bar, α-GalCer-treated mice. Representative dot plots of liver DC ($CD11c^+$ MHC class II^+ cells) at day 1 after α-GalCer or vehicle administration are shown in the left panels. The calculated percentages of liver DC are shown in the right. (b) BALB/c mice were treated with α-GalCer or vehicle. Hepatic MNC were prepared on day 0, 1, 3 and 7 and DC were isolated from liver MNC by a magnetic cell sorting system. For phenotypic analysis, liver DC were stained with phycoerythrin (PE)- or fluorescein isothiocyanate (FITC)-conjugated monoclonal antibodies (CD11c, CD40, CD80, CD86), and the expressions of these molecules were analyzed by flow cytometry. White bar, vehicle-treated mice; black bar, α-GalCer-treated mice. $*P < 0.05$ vs vehicle-treated mice, $\#P < 0.05$ vs non-treated mice. Representative histograms of the expressions of CD80, CD86 and CD40 on liver DC at day 1 after α-GalCer or vehicle administration are shown in the upper panels.

contrasts were tested with a Student's *t*-test with Welch's correction for unequal variance as needed.

RESULTS

α-GalCer administration inhibited CMS4 liver tumor mediated by NK cells

WE INITIALLY EXAMINED whether α-GalCer administration could induce antitumor effect against CMS4 liver tumor. As shown in Figure 1(a), no tumors were observed in the livers of α-GalCer-treated mice whereas large tumors were observed in the livers of vehicle-treated mice. The liver weight of the α-GalCer treatment group was significantly lighter than that of the vehicle treatment group (Fig. 1b). Depletion of NK cells significantly inhibited the antitumor efficacy of α-GalCer treatment (Fig. 1c), whereas depletion of neither $CD4^+$ nor $CD8^+$ T cells was inhibited (data not shown). These results suggested that administration of α-GalCer was therapeutic against CMS4 liver tumor and NK cells were the main effector cells in this antitumor immunity.

Administration of α-GalCer increased DC population in the liver MNC and activated DC functions

We investigated the population changes of DC in the liver MNC after α-GalCer or vehicle treatment. On day 1 after α-GalCer administration, liver DC proportion in α-GalCer-treated mice was higher than that in vehicle-treated mice (Fig. 2a). Liver DC proportion increased with the peak at 1 day after α-GalCer administration and the liver DC proportion at 7 days decreased to the same level with that from non-treated mice (Fig. 2a). In contrast, liver DC proportion in vehicle-treated mice exhibited weaker change than those in α-GalCer-treated mice (Fig. 2a). The liver DC number also exhibited increase at the peak of 1 day after α-GalCer administration whereas that from vehicle-treated mice exhibited no change (data not shown). We examined the CD40, CD80 and CD86 expressions of liver DC after administration of α-GalCer, which is an indicator of DC activation. On day 1 after α-GalCer administration, CD40, CD80 and CD86 on liver DC from α-GalCer-treated mice expressed more strongly than those from vehicle-treated mice (Fig. 2b). The expressions of all these molecules on liver DC increased with the peak at 1 day after α-GalCer administration and the expression levels of these molecules at 7 days decreased to the same levels on liver DC from non-treated mice (Fig. 2b). In contrast, the expressions of these molecules on liver DC exhibited weaker change in vehicle-treated mice.

Activated NK cells composed the major subpopulation of hepatic MNC that increased after α-GalCer treatment

We examined the population change of MNC from the livers after α-GalCer or vehicle administration. It is notable that NK cells strikingly increased in proportion after α-GalCer administration, but not after vehicle administration (Fig. 3a). In contrast, the NKT cells decreased at 1 and 3 days after α-GalCer administration and recovered at day 7 after α-GalCer administration. Both $CD4^+$ and $CD8^+$ T cells decreased in proportion after α-GalCer administration, but not after vehicle administration. We also examined the CD69 expressions of NK cells, which is an indicator of lymphocyte activation. The CD69 expressions on liver NK cells increased with the peak at 1 day and gradually decreased at 7 days after α-GalCer administration (Fig. 3b). In contrast, those did not change after vehicle administration. These results demonstrated that the activated NK cells were the major subpopulation of MNC that increased in the liver after α-GalCer administration.

$p53_{232-240}$ peptide-specific CTL were generated after α-GalCer treatment of liver tumor

We evaluated whether $p53_{232-240}$ peptide-specific CTL were generated after α-GalCer treatment of liver tumor. $CD8^+$ T cells were isolated from the spleen cells of treated mice and then co-cultured with syngeneic DC pulsed with $p53_{232-240}$ peptide strongly expressed on CMS4 cells. As shown in Figure 4(a), the number of

Figure 3 Activated natural killer (NK) cells composed the major subpopulation of hepatic mononuclear cells (MNC) that increased after α-galactosylceramide (α-GalCer) treatment. (a) BALB/c mice were treated with α-GalCer or vehicle. Hepatic MNC were prepared on days 0, 1, 3 and 7. NK cells, NKT cells, $CD4^+$ T cells and $CD8^+$ T cells in liver MNC were evaluated by flow cytometry. (b) The expressions of CD69 on liver NK cells were also evaluated by flow cytometry. White bar, vehicle-treated mice; black bar, α-GalCer-treated mice. $^*P < 0.05$ vs vehicle-treated mice.

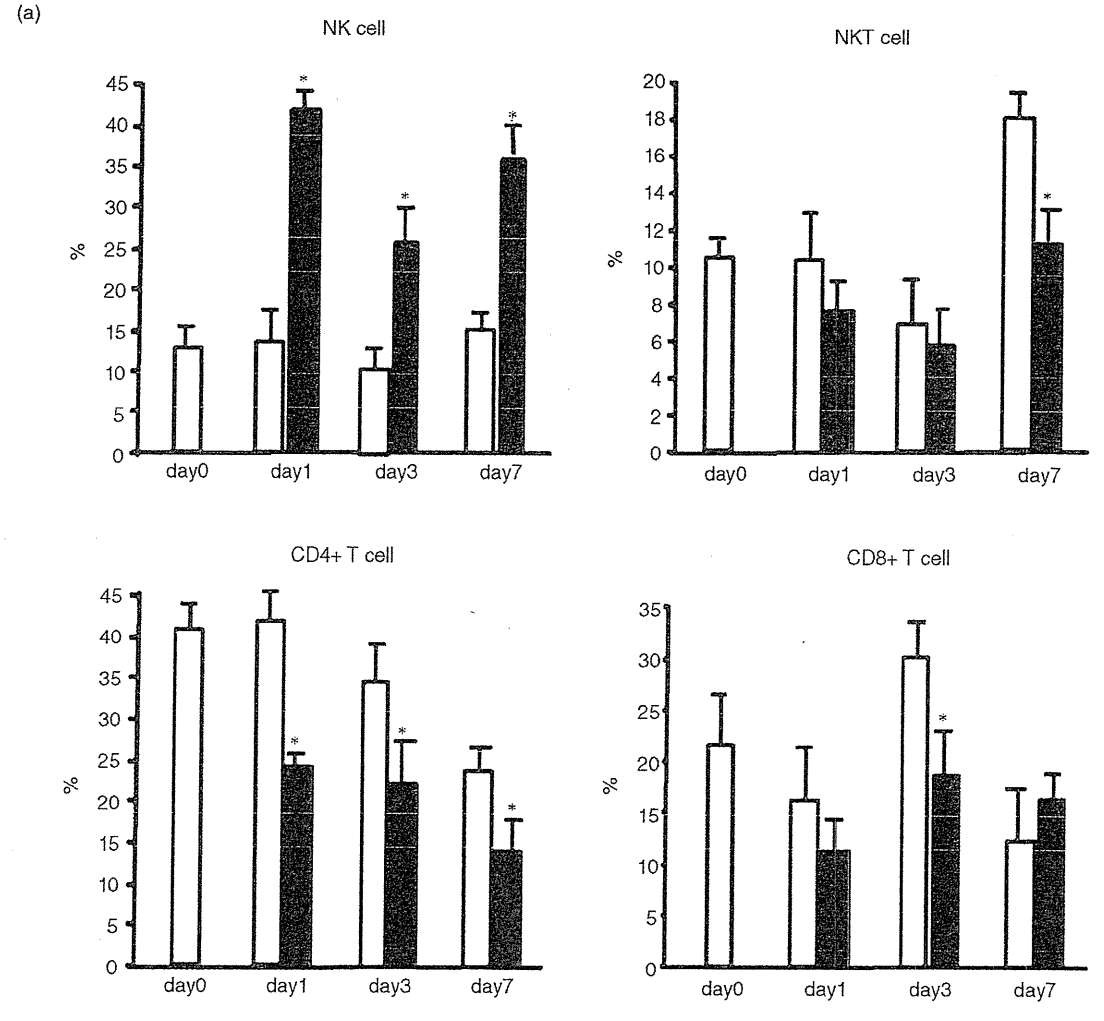

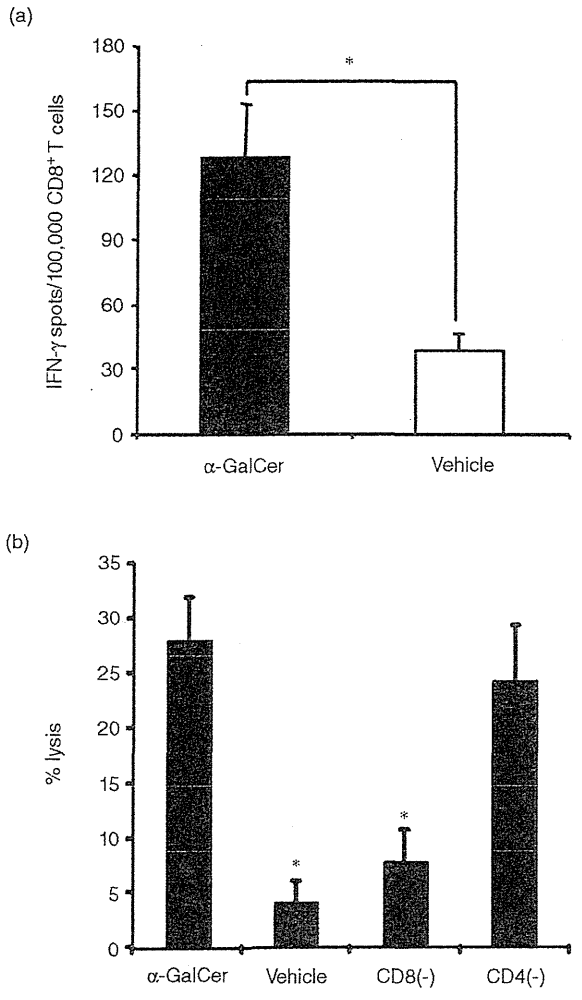

Figure 4 Evaluation of $p53_{232-240}$ peptide-specific $CD8^+$ cytotoxic T lymphocytes (CTL) in α-galactosylceramide (α-GalCer)-treated mice. (a) $CD8^+$ T cells were isolated from the spleen cells of treated mice 14 days after α-GalCer or vehicle treatment. The frequency of $p53_{232-240}$ peptide-specific $CD8^+$ CTL was evaluated by interferon (IFN)-γ enzyme-linked immunosorbent spot (ELISPOT) assay. The results are shown in spots/100 000 $CD8^+$ T cells; mean ± standard deviation of triplicate samples. $^*P < 0.05$. (b) Splenocytes from α-GalCer- or vehicle-treated mice were harvested 14 days after tumor inoculation and were analyzed for their ability to kill CMS4 cells in 4 h ^{51}Cr-release assays (effector cells/target cells ratio, 60:1). $CD4^+$ or $CD8^+$ T cells were depleted by magnetic sorting using CD4 or CD8 microbeads (Miltenyi Biotec), respectively. $CD8^-$, $CD8^+$ T-cell-depleted splenocytes. $CD4^-$, $CD4^+$ T-cell-depleted splenocytes. $^*P < 0.05$ vs the cytolytic activity of splenocytes from α-GalCer-treated mice.

IFN-γ spots (per 100 000 $CD8^+$ T cells) observed for T-cell responses against $p53_{232-240}$ peptide in α-GalCer-treated mice were significantly higher than that in vehicle-treated mice. These results suggested that strong $p53_{232-240}$ peptide-specific CTL were generated by α-GalCer treatment of liver tumor. Splenocytes from α-GalCer-treated mice displayed strong cytolytic activity against CMS4 cells, while those from vehicle-treated mice did not (Fig. 4b). $CD8^+$ T-cell-depleted splenocytes from α-GalCer-treated mice displayed significant weak cytolytic activity against CMS4 cells, but $CD4^+$ T-cell-depleted splenocytes did not. These results demonstrated that $CD8^+$ T cells (i.e. CTL) played essential roles in the cytolytic activity against CMS4 cells in α-GalCer-treated mice.

Systemic therapeutic antitumor immunity was induced by α-GalCer treatment of CMS4 liver tumor

Because strong $p53_{232-240}$ peptide-specific CTL were generated in α-GalCer-treated animals, we next chose to analyze whether the treatment of a CMS4 lesion in the liver would impact the progression of subcutaneous untreated CMS4 tumors. BALB/c mice were intrahepatically injected with CMS4 tumors and treated by administration of α-GalCer. Twenty-eight days later, 1×10^6 CMS4 cells or Colon26 cells were injected s.c. in the right flank. As shown in Figure 5(a), the non-treated CMS4 tumors in mice receiving α-GalCer treatment were completely rejected in all mice. The growth of non-treated Colon26 tumor in α-GalCer-treated mice was not inhibited (Fig. 5b). These results suggested that systemic CMS4-specific antitumor immunity could be induced by α-GalCer treatment. To confirm the involvement of CTL in this antitumor effect, we depleted $CD8^+$ T cells before re-challenge of CMS4 cells (s.c. injection of 1×10^6 CMS4 cells) in α-GalCer-treated mice bearing CMS4 liver tumor. On days 1 and 3 of re-challenge of CMS4 cells, anti-CD8 antibody (53–6.72 hybridoma, ATCC) was injected i.p. As shown in Figure 5(c), antitumor effect against re-challenged CMS4 subcutaneous tumor was diminished in $CD8^+$ T-cell-depleted mice. These results supported that $CD8^+$ T cells (i.e. CTL) play essential roles in the antitumor effect against re-challenge of CMS4 cells in α-GalCer-treated mice.

DISCUSSION

WE PREVIOUSLY DEMONSTRATED that administration of α-GalCer activated both NKT cells and NK cells in the liver, and that liver NK cells were the

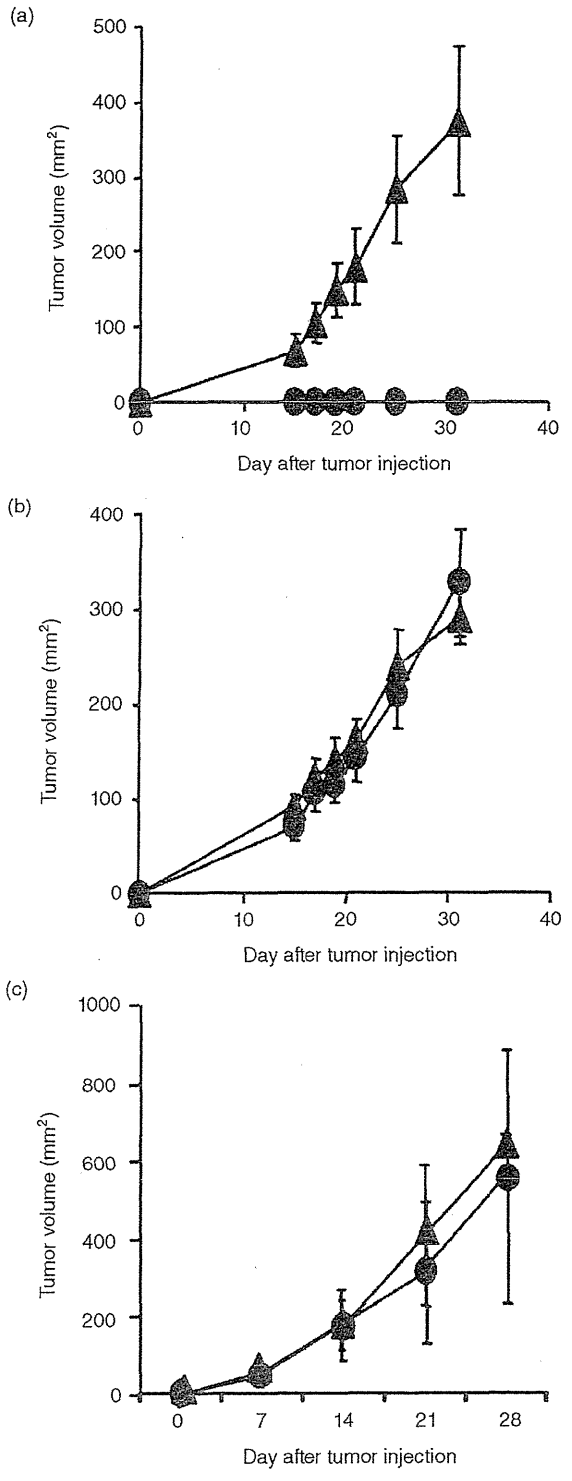

Figure 5 α-Galactosylceramide (α-GalCer) therapy results in the development of systemic antitumor immunity that protects distal tumor re-challenge. BALB/c mice were injected intrahepatically with CMS4 tumors. Twenty-four hours later, the mice were treated with α-GalCer. Twenty-eight days after treatment, α-GalCer-treated mice were re-challenged s.c. with 1×10^6 CMS4 cells (a) or Colon26 cells (b) in the right flank (all treatment groups, $n = 8$). To confirm the involvement of cytotoxic T lymphocytes (CTL) in this antitumor effect, we depleted $CD8^+$ T cells before re-challenge of CMS4 cells in α-GalCer-treated mice bearing CMS4 liver tumor (c). On days 1 and 3 of re-challenge of CMS4 cells, anti-CD8 antibody was injected i.p. Tumor size was assessed every 3 or 4 days after s.c. injection of tumor cells (on day 0). As control mice, naïve mice were injected s.c. with 1×10^6 CMS4 cells (a, $n = 8$; c, $n = 6$) or Colon26 cells (b) ($n = 8$) on day 0. (●) α-GalCer-treated mice, (▲) control mice. Each data point represents the mean tumor size ± standard deviations.

main effector cells to kill disseminated hepatoma cells injected from spleen in α-GalCer treatment.[4] In this study, we evaluated α-GalCer treatment in local injected liver tumor, and the α-GalCer treatment resulted in complete rejection of local liver tumor, which had a similar antitumor effect as α-GalCer in a previous metastatic liver tumor model. These findings suggested the ability of α-GalCer treatment to activate the liver NK cells efficiently, which may mainly contribute to eradication of local liver tumor cells. A normal liver contains lymphocytes that are usually enriched with NK and NKT cells; namely, 25% NK cells and 30% NKT cells in contrast to peripheral blood that contains only 10% NK and 5% NKT cells.[6,7] Thus, activation of innate immune cells, NK cells and NKT cells must be important to develop more effective immunotherapy against liver cancer. We believe that α-GalCer treatment must be a good candidate for human liver cancer treatment.

Recently, activated DC have been implicated in the activation of NKT and NK cells in both mice and humans,[1,5,8–12,22] suggesting that DC play crucial roles in the activation of abundant immune cells in the liver. To establish more efficient α-GalCer treatment in liver cancer, the precise mechanism of liver DC activation is needed. Our results demonstrated that the proportion of liver DC in liver MNC increased immediately and reached the peak 1 day after α-GalCer treatment. The infiltration of tumors by mature DC has been reported to correlate with a better prognosis in cancer patients.[23,24] Thus, the increase of liver DC by α-GalCer might contribute to generation of antitumor effect against liver cancer. The expressions of co-stimulatory

molecules on liver DC also increased early after administration of α-GalCer. IL-12 production from DC is key Th1-cytokine to enhance NK and CTL functionality,[25,26] IL-12 production from liver DC after α-GalCer treatment was significantly higher than that after vehicle treatment.[17] These results suggested that α-GalCer treatment resulted in rapid activation of liver DC, which might play important roles in activating liver NK cells and might contribute to the subsequent establishment of acquired immunity against liver cancer. Pillarisetty *et al.* identified new DC subsets, NK–DC, which presented in the liver of mice,[27] which may affect the interpretation of the activation of liver NK cells by α-GalCer. However, we previously demonstrated that α-GalCer had no direct effect on liver NK cells in mice.[4] These results supported the idea that α-GalCer activated liver DC, which activated the liver NK cells secondary.

Interferon-γ ELISPOT assay revealed that the frequency of $CD8^+$ T cells isolated from α-GalCer-treated mice in liver tumors in response to $p53_{232-240}$ peptide were much higher than that from vehicle-treated mice. Mayordomo *et al.* reported that immunization of $p53_{232-240}$ peptide-pulsed DC induced peptide-specific CTL in immunized mice that showed cytolytic activity against CMS4, p53 overexpressing cells.[18] In this study, ^{51}Cr-release assay demonstrated that $CD8^+$ T cell, not $CD4^+$ T cells, played essential roles in the cytolytic activity against CMS4 cells in α-GalCer-treated mice, which is consistent with the IFN-γ ELISPOT results. The detection of $p53_{232-240}$ peptide-specific CTL means the generation of CMS4 tumor-specific CTL after eradication of liver tumor by α-GalCer treatment. The activation of NKT cells was associated with an expansion of antigen-specific CTL, as might be expected if the DC that matured *in vivo* in response to NKT cells were capturing antigens.[28–31] Our results suggested that the activation of hepatic DC might be associated with the efficiency of generation of tumor antigen-specific CTL.

Additional experiments using an s.c. re-challenge with tumor demonstrated that α-GalCer treatment of liver tumors not only blocked treated CMS4 liver tumor progression but completely protected against consequent "recurrence" of that same tumor at a distant site. In contrast, Colon26 re-challenge tumor was not inhibited in treated mice, suggesting that CMS4-specific immunity was generated after liver tumor treatment. These results were consistent with the activation of acquired immunity evaluated by IFN-γ ELISPOT assay with increase of the frequency of $p53_{232-240}$ peptide-specific CTL. Taken together, we believe that α-GalCer treatment of liver tumors resulted in rejection of both local liver tumor and distant metastatic tumor.

In summary, we have shown that α-GalCer treatment activated both innate and acquired immune cells in the liver. These findings suggested that the use of α-GalCer might represent a particularly promising approach to suppress tumor growth and to promote regression of metastatic lesions in liver cancer patients.

ACKNOWLEDGMENTS

THIS WORK WAS supported by a Grant-in-Aid from the Ministry of Education, Culture, Sports, Science and Technology of Japan and a Grant-in-Aid for Research on Hepatitis and BSE from the Ministry of Health, Labour and Welfare of Japan.

REFERENCES

1 Kawano T, Cui J, Koezuka Y *et al.* CD1d-restricted and TCR-mediated activation of Vα14NKT cells by glycosylceramides. *Science* 1997; 278: 1626–9.
2 Fujii S, Shimizu K, Kronenberg M, Steinman RM. Prolonged IFN-γ- producing NKT response induced with alpha-galactosylceramide-loaded DCs. *Nat Immunol* 2002; 3: 867–74.
3 Gonzalez-Aseguinolaza G, de Oliveira C, Tomaska M *et al.* α-Galactosylceramide-activated Vα 14 natural killer T cells mediate protection against murine malaria. *Proc Natl Acad Sci USA* 2000; 97: 8461–6.
4 Miyagi T, Takehara T, Tatsumi T *et al.* CD1d-mediated stimulation of natural killer T cells selectively activates hepatic natural killer cells to eliminate experimentally disseminated hepatoma cells in murine liver. *Int J Cancer* 2003; 106: 81–9.
5 Giaccone G, Punt CJ, Ando Y *et al.* A phase I study of the natural killer T-cell ligand α-galactosylceramide (KRN7000) in patients with solid tumors. *Clin Cancer Res* 2002; 8: 3702–9.
6 Doherty DG, O'Farrelly C. Innate and adaptive lymphoid cells in human liver. *Immunol Rev* 2000; 174: 5–20.
7 Mehal WZ, Azzaroli F, Crispe IN. Immunology of the healthy liver: old questions and new insights. *Gatsroenterology* 2001; 120: 250–60.
8 Steinman RM. The dendritic cell system and its role in immunogenicity. *Annu Rev Immunol* 1991; 9: 271–96.
9 Hart DN. Dendritic cells: unique leukocyte populations which control the primary immune response. *Blood* 1997; 90: 3245–87.
10 Fernandez NC, Lozier A, Flament C *et al.* Dendritic cells directly trigger NK cell functions: cross-talk relevant in innate anti-tumor immune responses in vivo. *Nat Med* 1999; 5: 405–11.

11 Gerosa F, Baldani-Guerra B, Nisii C, Marchesini V, Carra G, Trinchieri G. Reciprocal activating interaction between natural killer cells and dendritic cells. *J Exp Med* 2002; 195: 327–33.
12 Ferlazzo G, Tsang ML, Moretta L, Melioli G, Steinman RM, Munz C. Human dendritic cells activate resting NK cells and are recognized via the NKp30 receptor by activated NK cells. *J Exp Med* 2002; 195: 343–51.
13 Piccioli D, Sbrana S, Melandri E, Valiante NM. Contact-dependent stimulation and inhibition of dendritic cells by natural killer cells. *J Exp Med* 2002; 195: 335–41.
14 Miller G, Lahrs S, Dematteo RP. Overexpression of interleukin-12 enables dendritic cells to activate NK cells and confer systemic antitumor immunity. *FASEB J* 2003; 17: 728–30.
15 Kawano T, Cui J, Koezuka Y *et al.* Natural killer-like nonspecific tumor cell lysis mediated by specific ligand-activated Vα14NKT cells. *Proc Natl Acad Sci USA* 1998; 95: 5690–3.
16 Kitamura H, Iwakabe K, Yahata T *et al.* The natural killer T (NKT) cell ligand α-galactosylceramide demonstrates its immunopoteniating effect by inducing interleukin (IL)-12 production by dendritic cells and IL-12 receptor expression on NKT cells. *J Exp Med* 1999; 189: 1121–8.
17 Sasakawa A, Tatsumi T, Takehara T *et al.* Activated liver dendritic cells generates strong acquired immunity in α-galctosylceramide treatment. *J Hepatol* 2009; 50: 1155–62.
18 Mayordomo JI, Loftus DJ, Sakamoto H *et al.* Therapy of murine tumors with p53 wild-type and mutant sequence peptide-based vaccines. *J Exp Med* 1996; 183: 1357–65.
19 Tatsumi T, Huang J, Gooding WE *et al.* Intratumoral delivery of dendritic cells engineered to secrete both interleukin(IL)-12 and IL-18 effectively treats local and distant disease in association with broadly reactive Tc1-type immunity. *Cancer Res* 2003; 63: 6378–86.
20 Uemura A, Takehara T, Miyagi T *et al.* Natural killer cell is a major producer of IFN-γ that is critical for the IL-12-induced anti-tumor effect in mice. *Cancer Immunol Immunother* 2010; 59: 453–63.
21 Yamaguchi S, Tatsumi T, Takehara T *et al.* Immunotherapy of murine colon cancer using receptor tyrosine kinase EphA2-derived peptide pulsed dendritic cell vaccines. *Cancer* 2007; 110: 1469–77.
22 Ferlazzo G, Munz C. NK cell compartments and their activation by dendritic cells. *J Immunol* 2004; 172: 1333–9.
23 Takagi S, Miyagawa S, Ichikawa E *et al.* Dendritic cells, T-cell infiltration, and Grp94 expression in cholangiocellular carcinoma. *Hum Pathol* 2004; 35: 881–6.
24 Iwamoto M, Shinohara H, Miyamoto A *et al.* Prognostic value of tumor-infiltrating dendritic cells expressing CD83 in human breast carcinomas. *Int J Cancer* 2003; 104: 92–7.
25 Kobayashi M, Fitz L, Ryan M *et al.* Identification and purification of natural killer cell stimulatory factors (NKSF), a cytokine with multiple biological effects on human lymphocytes. *J Exp Med* 1989; 170: 827–45.
26 Gately MK, Wolitzky AG, Quinn PM, Chizzonite R. Regulation of human cytolytic lymphocyte responses by interleukin-12. *Cell Immunol* 1992; 143: 127–42.
27 Pillarisetty VG, Katz SC, Bleier JI, Shah AB, DeMatteo RP. Natural killer dendritic cells have both antigen presenting and lytic function and in response to CpG produce IFN-γ via autocrine IL-12. *J Immunol* 2005; 174: 2612–18.
28 Fujii S, Shimizu K, Smith C, Bonifaz L, Steinman RM. Activation of natural killer T cells by α-galactosylceramide rapidly induces the full maturation of dendritic cells in vivo and thereby acts as an adjuvant for combined CD4 and CD8 T cell immunity to a coadministered protein. *J Exp Med* 2003; 198: 267–79.
29 Fujii S, Liu K, Smith C, Bonito AJ, Steinman RM. The linkage of innate to adaptive immunity via maturing dendritic cells in vivo requires CD40 ligation in addition to antigen presentation and CD80/86 costimulation. *J Exp Med* 2004; 199: 1607–18.
30 Hermans IF, Silk JD, Gileadi U, Salio M *et al.* NKT cells enhance CD4+ and CD8+ T cells responses to soluble antigen in vivo through direct interaction with dendritic cells. *J Immunol* 2003; 171: 5140–7.
31 Nishimura T, Kitamura H, Iwakabe K *et al.* The interface between innate and acquired immunity: glycolipid antigen presentation by CD1d-expressing dendritic cells to NKT cells induces the differentiation of antigen-specific cytotoxic T lymphocytes. *Int Immunol* 2000; 12: 987–94.

Amino Acid Substitution in the Core Protein has no Impact on Relapse in Hepatitis C Genotype 1 Patients Treated With Peginterferon and Ribavirin

Yuko Inoue,[1] Naoki Hiramatsu,[1]* Tsugiko Oze,[1] Takayuki Yakushijin,[1] Kiyoshi Mochizuki,[1] Kazuto Fukuda,[2] Eiji Mita,[3] Yoshimichi Haruna,[4] Atsuo Inoue,[4] Yasuharu Imai,[2] Atsushi Hosui,[1] Takuya Miyagi,[1] Yuichi Yoshida,[1] Tomohide Tatsumi,[1] Shinichi Kiso,[1] Tatsuya Kanto,[1] Akinori Kasahara,[1] Tetsuo Takehara,[1] and Norio Hayashi[5]

[1]*Department of Gastroenterology and Hepatology, Osaka University Graduate School of Medicine, Suita, Japan*
[2]*Ikeda Municipal Hospital, Ikeda, Japan*
[3]*National Hospital Organization Osaka National Hospital, Osaka, Japan*
[4]*Osaka General Medical Center, Osaka, Japan*
[5]*Kansai Rousai Hospital, Amagasaki, Japan*

Previous reports demonstrated that amino acid (aa) substitutions in the hepatitis C virus (HCV) core protein are predictors of non-virological responses to pegylated interferon (Peg-IFN) and ribavirin combination therapy. The aim of this study was to investigate the impact of core aa substitutions on viral kinetics during the treatment and relapse after the treatment. The 187 patients with HCV genotype 1 enrolled in this study were categorized into four groups according to core aa substitution patterns: double-wild group (n = 92), Arg70/Leu91; 70-mutant group (n = 42), Gln70/Leu91; 91-mutant group (n = 31), Arg70/Met91; and double-mutant group (n = 22), Gln70/Met91. The relationship between the core aa substitutions and the virological response was examined. Multivariate logistic regression analyses showed that substitution at aa 70 was significantly associated with a poor virological response during the first 12 weeks (decline of <1 log from baseline at week 4, <2 log at week 12), and substitution at aa 91 was significantly associated with detectable HCV RNA at week 24. With respect to relapse, only the ribavirin exposure (odds ratio (OR), 0.77; 95% confidence interval (CI), 0.60–0.98) and HCV RNA disappearance between weeks 13 and 24 (OR, 23.69; 95% CI, 5.44–103.08) were associated independently with relapse, with no correlation being found with the core aa substitutions and relapse. In conclusion, the results showed that core aa substitutions can be strong predictive factors at pretreatment of the non-response, but not for relapse, for virological responders with HCV RNA disappearance during treatment. *J. Med. Virol. 83:419–427, 2011.*

KEY WORDS: amino acid substitution; core protein; hepatitis C virus; peginterferon and ribavirin combination therapy; relapse

INTRODUCTION

The current standard of care for chronic hepatitis C patients is combination therapy using pegylated interferon (Peg-IFN) and ribavirin [Anonymous, 2002; Strader et al., 2004; Dienstag and McHutchison, 2006]. However, the treatment outcome in response to this combination therapy among patients infected with hepatitis C virus (HCV) genotype 1 is still unsatisfactory and the chance of sustained virological response ranges from 42% to 52% [Manns et al., 2001; Fried et al., 2002; Hadziyannis et al., 2004]. Therefore, tailoring treatment regimens for individual patients has become an important issue.

Grant sponsor: Ministry of Health Labor and Welfare of Japan (Research on Hepatitis and BSE); Grant sponsor: Scientific Research from the Ministry of Education, Science, and Culture of Japan.

*Correspondence to: Naoki Hiramatsu, MD, PhD, Department of Gastroenterology and Hepatology, Osaka University Graduate School of Medicine, 2-2 Yamadaoka, Suita, Osaka 565-0871, Japan. E-mail: hiramatsu@gh.med.osaka-u.ac.jp

Accepted 20 September 2010

DOI 10.1002/jmv.21975

Published online in Wiley Online Library (wileyonlinelibrary.com).

Outcome of therapy is influenced by various factors. Some host factors, such as age, sex, body weight, insulin resistance, and liver fibrosis have been reported as pretreatment factors affecting virological response to this combination therapy [Manns et al., 2001; Fried et al., 2002; Hadziyannis et al., 2004; Romero-Gomez et al., 2005]. Recently, several genome-wide association studies identified single nucleotide polymorphisms (SNPs) near the interleukin (IL)-28B gene, which encodes interferon (IFN) lambda-3, as associated with response to Peg-IFN plus ribavirin treatment among patients infected with HCV of European [Suppiah et al., 2009], African [Ge et al., 2009], and Asian ancestry [Tanaka et al., 2009]. These studies suggest that host genetic variants may be associated strongly with response to IFN-alpha-based therapy. However, the ethical problem to perform host genetic search for all patients remains, and the sustained virological response rate is only 48–69% in patients having favorable IL-28B genotype to this combination therapy [Thompson et al., 2010].

Response-guided therapy is a dynamic approach to management of chronic hepatitis C patients based on the virological response at weeks 4 and 12 of treatment. At present, it is regarded as an excellent strategy for optimizing the treatment duration for individual patients. Earlier HCV RNA disappearance has been shown to lead to a higher sustained virological response rate [Ferenci et al., 2005; Berg et al., 2006; McHutchison et al., 2009], while patients without an early virological response, defined as showing an at least 2 log decrease from the baseline of HCV RNA levels at week 12 is recommended for discontinuing the treatment under the current guidelines [Anonymous, 2002; Strader et al., 2004; Dienstag and McHutchison, 2006].

In addition to viral kinetics during treatment, other viral factors have also been reported to be associated with this combination therapy outcome [Manns et al., 2001; Fried et al., 2002; Hadziyannis et al., 2004; Shirakawa et al., 2008]. Previous studies indicated that amino acid (aa) 70 and/or 91 substitutions in the HCV core protein were independent pretreatment predictors of null or weak response to this combination therapy in genotype 1 patients [Akuta et al., 2007b,c]. The HCV core protein has been reported to inhibit signal transducer and activator of transcription (STAT)-1 phosphorylation, and disrupt the normal IFN-stimulated transcriptional response to viral infection [Lin et al., 2006]. It is supposed that the HCV core region might be associated with resistance to IFN therapy involving the Janus activated kinase (Jak)-STAT signaling cascade [Blindenbacher et al., 2003; Bode et al., 2003; Melen et al., 2004; de Lucas et al., 2005]. Recently, Okanoue et al. [2009] have demonstrated that wild type of core aa 70 and 91 are important for positive prediction of the virological response. However, the impact of core aa substitutions on the extent of HCV RNA decline during the treatment or virological relapse after completion of treatment has not yet been investigated in detail. Approximately 30% of genotype 1 patients who become HCV RNA negative at the end of the treatment will experience relapse [Hadziyannis et al., 2004]. Being able to distinguish between end-of-treatment responders with a high probability of relapse and those with a low probability of relapse will be useful in reducing relapse rates and improving treatment outcome.

The aim of this study was to evaluate the impact of aa substitutions in the HCV core protein on viral kinetics and virological relapse in patients with HCV genotype 1 treated by Peg-IFN alpha-2b and ribavirin combination therapy.

PATIENTS AND METHODS

Patient Selection and Study Design

Patients considered to be eligible for this study were those who were infected with HCV genotype 1, had a viral load more than 10^5 IU/ml, had started Peg-IFN alpha-2b (Schering-Plough K.K. Tokyo, Japan) and ribavirin (Schering-Plough K.K.) combination therapy from December 2005 to June 2008 at Osaka University Hospital and three other medical institutions taking part in the Osaka Liver Forum, and had been examined with respect to the aa sequences at positions 70 and 91 in the HCV core protein with pretreatment serum samples. Patients with the following criteria were excluded: hepatitis B virus or human immunodeficiency virus co-infection; decompensated liver disease; severe cardiac, renal, hematological, or chronic pulmonary disease; poorly controlled psychiatric disease; poorly controlled diabetes; and immunologically mediated disease. As a result of screening at the institutions concerned, 187 patients with HCV genotype 1 were enrolled in this study. Liver biopsy had been performed within 12 months prior to the treatment, and histological results were classified according to the METAVIR scoring system [Bedossa and Poynard, 1996].

Written informed consent was obtained from each patient, and the study protocol was reviewed and approved according to the ethical guidelines of the 1975 Declaration of Helsinki by Institutional Review Boards at the respective sites.

Peg-IFN alpha-2b and ribavirin dosages were based on body weight according to the manufacturer's instructions: Peg-IFN alpha-2b was given subcutaneously weekly (45 kg or less, 60 μg/dose; 46–60 kg, 80 μg/dose; 61–75 kg, 100 μg/dose; 76–90 kg, 120 μg/dose; and 91 kg or more, 150 μg/dose), and ribavirin was given orally daily (60 kg or less, 600 mg/day; 61–80 kg, 800 mg/day; and 81 kg or more, 1,000 mg/day). The drug doses were also modified based on the manufacturer's instructions according to the severity of the adverse hematologic effects.

Detection of Amino Acid Substitutions in Core Region

The nucleotide sequence encoding aa 1–191 (the core protein of HCV) was analyzed by direct sequencing as described by Akuta et al. [2005, 2007b]. In brief, HCV

RNA was extracted from the serum samples and converted to cDNA and two nested rounds of polymerase chain reaction (PCR) were performed. Primers used in the PCR were as follows: the first PCR was performed using cc11 (sense, 5′-GCC ATA GTG GTC TGC GGA AC-3′) and e14 (antisense, 5′-GGA GCA GTC CTT CGT GAC ATG-3′) primers. The second PCR was performed using cc9 (sense, 5′-GCT AGC CGA GTA GTG TT-3′) and e14 (antisense) primers. All samples were denatured initially at 95°C for 15 min. The 35 cycles of amplification were set as follows: denaturation for 1 min at 94°C, annealing of primers for 2 min at 55°C, and extension for 3 min at 72°C with an additional 7 min for extension. Then 1 μl of the first PCR product was transferred to the second PCR reaction. The conditions for the second PCR were the same as the first PCR, except that the second PCR primers were used instead of the first PCR primers. The amplified PCR products were purified by the QIA quick PCR Purification Kit (Qiagen, Tokyo, Japan) after agarose gel electrophoresis and then used for direct sequencing. Dideoxynucleotide termination sequencing was performed with the Big Dye Deoxy Terminator Cycle Sequencing Kit (Perkin–Elmer, Tokyo, Japan). The obtained nucleotide and amino acid sequences were compared with the prototype sequence of genotype 1b HCV-J (GenBank Accession No. D90208) [Kato et al., 1990]. Wild types virus encoded arginine (Arg) and leucine (Leu) at aa 70 and 91, respectively, and the aa substitutions were glutamine (Gln) or histidine (His) at aa 70 and methionine (Met) at aa 91. If the intensities of the band were similar, the case was regarded as competitive. Two patterns of mutant and competitive were labeled as mutant. In this study, patients were categorized into four groups according to aa substitution patterns: double-wild group, Arg70/Leu91; 70-mutant group, Gln or His70/Leu91; 91-mutant group, Arg70/Met91; and double-mutant group, Gln or His70/Met91.

Virological Tests

Serum HCV RNA level was quantified by PCR assay (COBAS Amplicor HCV Monitor Test v2.0, Chugai-Roche Diagnostics, Tokyo, Japan), with a sensitivity limit of 5,000 IU/ml and a dynamic range from 5,000 to 5,000,000 IU/ml.

Serum HCV RNA was assessed by qualitative PCR assay (COBAS Amplicor HCV Test v2.0, Chugai-Roche Diagnostics), with a detection limit of 50 IU/ml.

Efficacy Assessments

Patients who achieved negative HCV RNA at week 12 were defined as having a complete early virological response. Patients who became HCV RNA negative between weeks 13 and 24 were defined as having a late virological response. According to the established guidelines, the treatment was considered to have failed if the patients showed an insufficient virological response at week 12 (a detectable HCV RNA and a decrease of <2 log from the baseline level) or at week 24 (a detectable HCV RNA), and therapy was discontinued. The end-of-treatment response was defined as undetectable HCV RNA at week 48. Patients with end-of-treatment response and undetectable HCV RNA 24 weeks after completion of therapy were defined as having sustained virological response. Relapse was defined as a case in which HCV RNA had been undetectable at the end-of-treatment, but detectable during the 24-week follow-up after the treatment.

Drug Exposure

The amounts of Peg-IFN alpha-2b and ribavirin actually taken by each patient during the treatment period were evaluated by reviewing the medical records. The mean doses of both drugs were calculated individually as averages on the basis of body weight at baseline; Peg-IFN alpha-2b expressed as μg/kg/week and ribavirin as mg/kg/day.

Data Collection

The medical records were retrospectively reviewed and the factors necessary for this examination were extracted: age, sex, body weight, body mass index (BMI), basic laboratory assessments, liver histology, quantitative and qualitative HCV RNA, dose of Peg-IFN alpha-2b and ribavirin received at each administration, and the response to treatment.

Statistical Analysis

Continuous variables are reported as the mean with standard deviation (SD) or median level, while categorical variables are shown as the count and proportion. In univariate analysis, the Mann–Whitney *U*-test (between two groups) or Kruskal–Wallis test (among more than three groups) was used to analyze continuous variables, while chi-squared and Fisher's exact tests were used for analysis of categorical data. For all tests, two-sided *P* values were calculated, and the results were considered statistically significant if $P < 0.05$. Variables that achieved statistical significance ($P < 0.05$) or marginal significance ($P < 0.10$) on univariate analysis were subjected to multivariate logistic regression analysis. Stepwise and multivariate logistic regression models were used to explore the independent factors that could be used to predict a virological response. Statistical analysis was performed using the SPSS program for Windows, version 15.0J (SPSS, Chicago, IL).

RESULTS

Baseline Characteristics of Study Groups

The total study population was predominately male (55.6%), with a mean age of 56.2 years. The baseline characteristics of all patients and the four study groups according to core aa substitution patterns are shown in Table I. Mean age of patients in the double-mutant group was higher than the other three groups ($P = 0.003$). More patients in the double-wild group had

TABLE I. Baseline Demographic and Viral Characteristics of Patients

Characteristic	Total (n = 187)	Double-wild (n = 92)	70-Mutant (n = 42)	91-Mutant (n = 31)	Double-mutant (n = 22)	P value[a]
Age (years)	56.2 ± 9.3	55.7 ± 9.2	57.0 ± 9.8	52.4 ± 9.9	61.8 ± 4.7	0.003
Sex (male/female)	104/83	51/41	26/16	18/13	9/13	0.444
Body weight (kg)	60.9 ± 11.6	60.9 ± 11.7	62.2 ± 11.7	62.5 ± 13.2	56.0 ± 7.5	0.193
Body mass index (kg/m^2)	22.8 ± 3.1	22.8 ± 3.0	22.8 ± 3.1	23.1 ± 3.6	22.1 ± 2.4	0.627
Past IFN therapy (naïve/experienced)	118/69	45/47	34/8	20/11	19/3	<0.001
HCV RNA (×10^3 IU/ml)[b]	1,700	2,100	1,400	1,500	1,230	0.122
Fibrosis (0–2/3–4)[c]	105/29	56/11	22/6	14/7	13/5	0.366
Activity (0–1/2–3)[d]	83/50	42/24	18/10	11/10	12/6	0.771
White blood cell (×10^6/l)	4,980 ± 1,520	4,990 ± 1,420	5,180 ± 1,760	4,890 ± 1,430	4,660 ± 1,560	0.795
Red blood cell (×10^{12}/l)	4.34 ± 0.46	4.33 ± 0.46	4.41 ± 0.52	4.39 ± 0.42	4.18 ± 0.32	0.145
Hemoglobin (g/dl)	13.9 ± 1.4	13.9 ± 1.4	14.0 ± 1.7	14.2 ± 1.4	13.5 ± 1.1	0.253
Platelet (×10^9/l)	161 ± 54	167 ± 49	165 ± 65	154 ± 60	138 ± 30	0.067
ALT (IU/l)	74 ± 61	73 ± 67	79 ± 56	81 ± 64	57 ± 37	0.263
γ-GTP (IU/l)	62 ± 74	47 ± 54	81 ± 89	70 ± 93	78 ± 78	0.032

IFN, interferon; HCV, hepatitis C virus; ALT, alanine aminotransferase; γ-GTP, gamma-glutamyl transpeptidase.
[a]P value for comparison among double-wild, 70-mutant, 91-mutant, and double-mutant.
[b]Values expressed as median.
[c]Data for 53 patients are missing.
[d]Data for 54 patients are missing.

been treated previously for HCV infection ($P < 0.001$). Patients in the double-wild group had significantly lower gamma-glutamyl transpeptidase (γ-GTP) levels ($P = 0.032$).

Progress of Patients

The progress of patients in this study is shown in Figure 1. Of the 187 patients, 183 completed 4 weeks of treatment. Among them, 133 were assessed based on HCV RNA dynamics between baseline and week 4. Those completing 12 weeks of treatment totaled 181, of which 154 were assessed for HCV RNA dynamics between baseline and week 12. Those completing 24 weeks of treatment totaled 153, and all were assessed for HCV RNA quantitatively or qualitatively at week 24. Those completing 48 weeks of treatment totaled 114. These 114 patients and the 55 patients who had discontinued treatment because of treatment failure entered a follow-up period. Among these 169 patients, 164 completed 24 weeks follow-up and the sustained virological response (SVR) rate

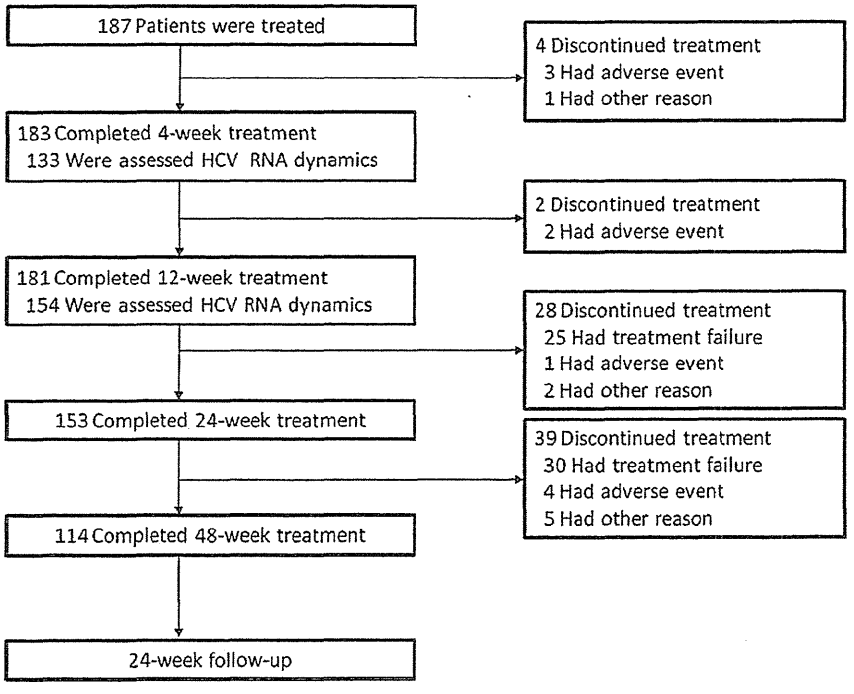

Fig. 1. Treatment and follow-up of the study patients. Treatment was discontinued for patients with <2 log decrease from the baseline HCV RNA level at week 12 or detectable HCV RNA at week 24.

TABLE II. Multivariate Analysis for Factors Associated With <1 log Decrease in HCV RNA Level at Week 4, <2 log Decrease at Week 12, Detectable HCV RNA at Week 24, and Relapse After Treatment

Factor	Category	Odds Ratio	95% CI	*P* value
HCV RNA <1 log decrease at week 4				
White blood cells ($\times 10^6$/l)	<5,000/5,000≤	—	—	NS
γ-GTP (IU/l)	<40/40≤	—	—	NS
Peg-IFN dose (μg/kg/week)	By 0.1 μg/kg/week	0.80	0.67–0.97	0.020
Core aa 70	Wild/mutant	1/2.80	1.16–6.75	0.022
HCV RNA <2 log decrease at week 12				
γ-GTP (IU/l)	<40/40≤	—	—	NS
Peg-IFN dose (μg/kg/week)	By 0.1 μg/kg/week	—	—	NS
Core aa 70	Wild/mutant	1/2.72	1.09–6.78	0.032
Detectable HCV RNA at week 24				
Platelet ($\times 10^9$/l)	<150/150≤	—	—	NS
γ-GTP (IU/l)	<40/40≤	1/2.46	1.02–5.95	0.045
Core aa 91	Wild/mutant	1/4.11	1.73–9.78	0.001
Relapse after treatment				
Ribavirin dose (mg/kg/day)	By 1 mg/kg/day	0.77	0.60–0.98	0.036
Virological response	Complete early virological response/late virological response	1/23.69	5.44–103.08	<0.001

CI, confidence interval; NS, not significant difference; γ-GTP, gamma-glutamyl transpeptidase; Peg-IFN, pegylated interferon; aa, amino acid.

was 48.2% (79/164), based on per-protocol set. Among the 106 patients who had an end-of-treatment response and completed follow-up, 27 showed relapse during the follow-up period; the relapse rate was 25.5% (27/106).

IMPACT OF CORE-RELAPSE AFTER TREATMENT (TABLE II)

Impact of core aa substitutions on <1 log viral decrease rate at week 4, <2 log at week 12, detectable HCV RNA at week 24, and virological relapse after treatment (Table II).

The impact of core aa substitutions on <1 log viral decrease rate at week 4, <2 log at week 12, detectable HCV RNA at week 24, and virological relapse after treatment (Table II).

The impact of the core aa substitutions on <1 log viral decrease at week 4, which is a predictor of non-sustained virological response; fewer than 5% of patients without 1 log decrease at week 4 had an sustained virological response [McHutchison et al., 2009] was examined. Among the 133 patients who completed 4 weeks of treatment, 31 failed to show a ≥1 log decrease of HCV RNA level at week 4. Univariate analysis for factors associated with <1 log decrease of HCV RNA level at week 4 was performed on the following variables: age, sex, body weight, BMI, history of past IFN therapy, baseline HCV RNA level, histological fibrosis and activity, white blood cell count, red blood cell count, hemoglobin level, platelet count, alanine aminotransferase (ALT) level, γ-GTP level, dose exposure of Peg-IFN and ribavirin, and aa substitutions in the HCV core protein. The results indicated that pretreatment white blood cell count, γ-GTP level, the mean dose of Peg-IFN during the first 4 weeks of treatment and single-spot substitution in the HCV RNA core position at aa 70 contributed to a <1 log decrease of HCV RNA level at week 4. Analysis of these factors by multivariate logistic regression analysis showed that substitution of aa 70 (odds ratio (OR) 2.80, 95% confidence interval (CI) 1.16–6.75, $P = 0.022$) as well as the mean dose of Peg-IFN (OR 0.80, 95% CI 0.67–0.97, $P = 0.020$) was independently associated with viral decline (<1 log) at week 4.

Next, the impact of the core aa substitutions on <2 log viral decrease rate at week 12, which is presently considered to be the most reliable predictor of non-sustained virological response [Fried et al., 2002; Davis et al., 2003] was examined. Among the 154 patients who completed 12 weeks of treatment, 25 failed to show a ≥2 log decrease of HCV RNA level at week 12. Univariate analysis was performed on the same factors in the preceding examination. As a result, pretreatment γ-GTP level, the mean dose of Peg-IFN during the first 12 weeks of treatment and single-spot substitution in the HCV RNA core position at aa 70 contributed to a <2 log decrease of the HCV RNA level. These factors were then analyzed by multivariate logistic regression analysis; only substitution of aa 70 (OR 2.72, 95% CI 1.09–6.78, $P = 0.032$) was found to be independently associated with an insufficient virological response (<2 log HCV RNA decrease from baseline level) at week 12.

The impact of the core aa substitutions on detectable HCV RNA at week 24, which is another non-sustained virological response predictor [Davis et al., 2003] was also examined. Among 153 patients who completed 24 weeks of treatment, 30 still had detectable HCV RNA at week 24. Univariate analysis revealed that pretreatment platelet count, γ-GTP level, and single-spot substitution in the HCV RNA core position at aa 91 contributed to the HCV RNA remaining positive. Multivariate logistic regression analysis, using these factors, indicated that substitution of aa 91 (OR 4.11, 95% CI 1.73–9.78, $P = 0.001$) as well as γ-GTP level (>40 IU/l) (OR 2.46, 95% CI 1.02–5.95, $P = 0.045$) was

independently associated with detectable HCV RNA at week 24.

Next, the factors associated with virological relapse after the treatment was examined. Univariate analysis was performed on the virological response (complete early virologival response or late virological response) in addition to the factors in the preceding examination, revealing the mean dose of ribavirin during the full treatment period and a late virological response, but not aa substitutions (single-spot substitution in the HCV RNA core position at aa 70, $P = 0.467$; aa 91, $P = 0.776$).

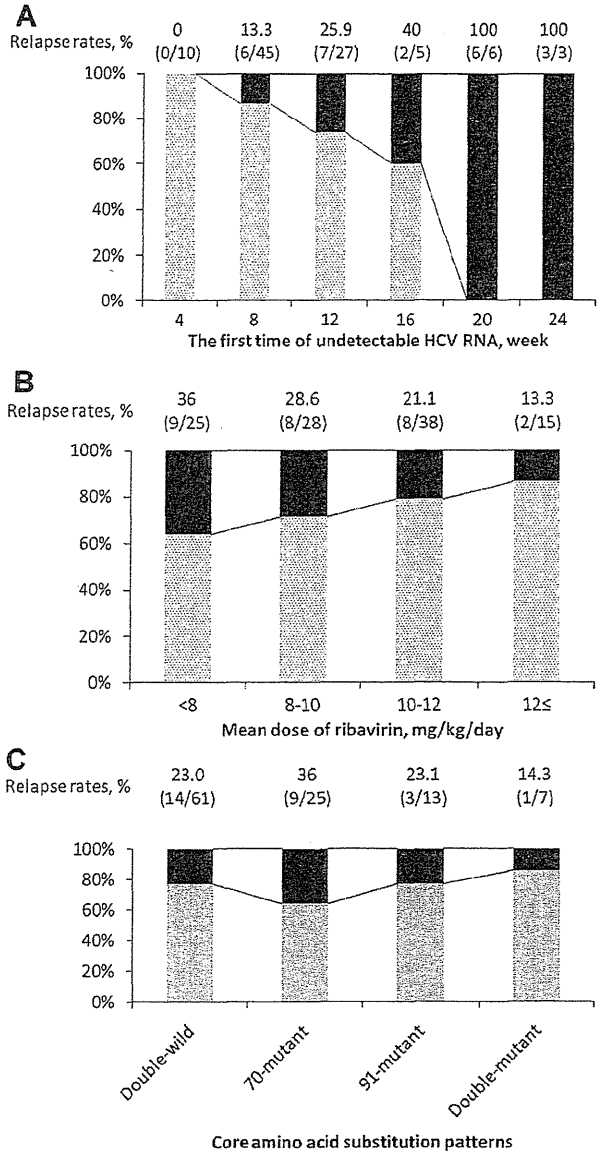

Fig. 2. Relapse rates according to the timing of HCV RNA disappearance (**A**), mean ribavirin dose (**B**), and core amino acid substitution patterns (**C**) in patients who had end-of-treatment response and completed 24-week follow-up. Relapse rates are shown as percentages and the number of patients with relapse in relation to the total number of patients examined is shown at the top of each column. Gray bar, sustained virological response; black bar, relapse.

These factors were analyzed by multivariate logistic regression analysis. This analysis revealed that the mean ribavirin dose (OR 0.77, 95% CI 0.60–0.98, $P = 0.036$) and a late virological response (OR 23.69, 95% CI 5.44–103.08, $P < 0.001$) were independently associated with relapse.

Relapse Rates According to the Timing of HCV RNA Disappearance, Ribavirin Dose, and Core aa Substitution Patterns

The relapse rates were indicated according to the time to the first non-detection of HCV RNA, mean ribavirin dose and core aa substitution patterns (Fig. 2). The relapse rate was 0% (0/10) in patients with undetectable HCV RNA during 1–4 weeks, and increased 13.3% (6/45) during 5–8 weeks, 25.9% (7/27) during 9–12 weeks, 40% (2/5) during 13–16 weeks, 100% (6/6) during 17–20 weeks, and 100% (3/3) during 21–24 weeks (Fig. 2A). Similarly, the relapse rates increased as the mean ribavirin dose decreased; 13.3% (2/15) in patients receiving ≥12 mg/kg/day of ribavirin, 21.1% (8/38) at 10–12 mg/kg/day, 28.6% (8/28) at 8–12 mg/kg/day, and 36% (9/25) at <8 mg/kg/day (Fig. 2B). On the other hand, the relapse rates were similar among the four core aa substitution patterns; 23.0% (14/61) in patients in the double-wild group, 36% (9/25) in 70-mutant group, 23.1% (3/13) in 91-mutant group, and 14.3% (1/7) in double-mutant group (Fig. 2C). In the subgroup of patients receiving <10 mg/kg/day of ribavirin, no significant difference of the relapse rates was observed between double-wild group and 70-mutant and/or 91-mutant group (31.3% (10/32) in double-wild group vs. 33.3% (7/21) in 70-mutant and/or 91-mutant group), and also in the patients receiving ≥10 mg/kg/day of ribavirin (13.8% (4/29) in double-wild group vs. 25% (6/24) in 70-mutant and/or 91-mutant group) (Fig. 3). Among patients with complete early virological response, the relapse rates were also similar between double-wild group and 70-mutant and/or 91-mutant group (13.7% (7/51) in double-wild vs. 18.4% (7/38) in 70-mutant and/or 91-mutant group). The impact of core aa substitutions on relapse rates in patients with late virological response could not be assessed because of the small number of patients.

DISCUSSION

Kobayashi et al. [2010] investigated the clinical and virological factors influencing these core aa substitutions in patients infected with HCV genotype 1 who had not received antiviral therapy, and found that HCV variants with wild type of core aa 70 and 91 significantly decreased with age, while those with the mutant type of core aa 70 and/or 91 significantly increased with age. Furthermore, they demonstrated that the proportion of patients with the mutant type of core aa 70 HCV variant significantly increased with an elevated γ-GTP level and a decrease in platelet counts. In this study, the significant differences of baseline demographics between patient groups according to core aa substitution pat-

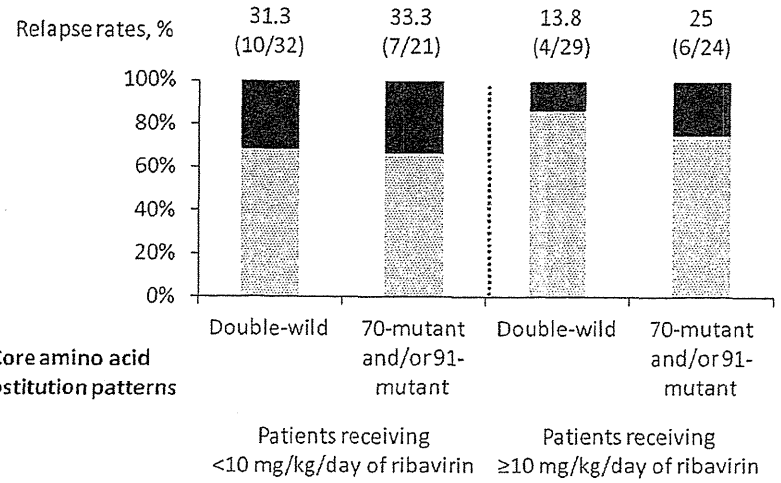

Fig. 3. Relapse rates according to core amino acid substitution patterns in patients receiving <10 mg/kg/day and receiving ≥10 mg/kg/day of ribavirin. Relapse rates are shown as percentages and the number of patients with relapse in relation to the total number of patients examined is shown at the top of each column. Gray bar, sustained virological response; black bar, relapse.

terns were similarly found in age, platelet count, and γ-GTP level. Accordingly, this study cohort had no specific bias and seems to reflect the natural background of the patients according to the HCV variance. In this study, the impact of HCV core aa substitutions on the virological response were evaluated by multivariate analysis, in order to resolve the bias of patient background factors among the groups classified according to the core aa substitution patterns. Recently, Abe et al. [2010] reported that the human genotype of the rs8099917 SNP at the IL28B locus was associated with lower γ-GTP level and viral wild type of core aa 70 and 91. Possibly these differences of IL28B genotype may influence the difference of patient background factors. Further studies are needed to clarify the relationship between human genetic variation and HCV core amino acid substitutions.

The HCV core protein has been reported to have an effect on a variety of cellular functions [Lai and Ware, 2000; Joo et al., 2005; Ariumi et al., 2007; Waris et al., 2007; Osna et al., 2008]. Currently, aa substitutions in the HCV core region has been thought to be related with outcome of antiviral therapy [Akuta et al., 2005; Donlin et al., 2007] and also the development of hepatocellular carcinoma [Akuta et al., 2007a; Hu et al., 2009]. Importance of core aa substitutions, especially at aa 70 and 91, comes to be recognized, and the new method to detect these substitutions easily has been proposed [Nakamoto et al., 2009]. As for the mechanism of antiviral activity on core aa substitutions, Ikeda et al. [2010] showed that core aa substitutions were not associated with intracellular antiviral response to IFN-alpha by in vitro analysis. The mechanism of antiviral activity and hepatocarcinogenesis on core aa substitutions has not been elucidated enough, so far. Further in vitro studies will be needed to clarify this.

Previous studies showed that patients with substitution of core aa 70 often had slow or no decrease in HCV RNA levels during the early phase of IFN-alpha treatment [Akuta et al., 2005, 2007b,c; Donlin et al., 2007]. Consistent with these reports, multivariate analysis in this study revealed that substitution of core aa 70 could be independently associated with insufficient viral decline during the first 12 weeks after the treatment (decline of <1 log from baseline at week 4, <2 log at week 12). This suggests that patients with substitution of core aa 70 are likely to fail to have a sustained virological response. On the other hand, dose exposure of Peg-IFN during the first 4 weeks of treatment was also independently linked to a minimal decline in HCV RNA (<1 log) at week 4 in this study. This suggests that maintaining the dose of Peg-IFN as high as possible until the disappearance of HCV RNA can help avoid treatment failure [McHutchison et al., 2002; Oze et al., 2009], especially in patients with substitution of core aa 70. On the other hand, substitution of core aa 91 was independently associated with detectable HCV RNA at week 24. This suggests that patients with substitution of core aa 91 are likely to achieve non-sustained virological response even if they had a ≥2 log decline in the HCV RNA level at week 12. The reason for the difference of the impact on virological response is not yet clear.

Multivariate logistic regression analysis also showed that the dose exposure of ribavirin during the full treatment period and having late virological response were independently associated with relapse. As for ribavirin exposure, it has been previously demonstrated that the relapse rate among patients responding to the treatment showed a decline in relation to the increase in the dose of ribavirin [Hiramatsu et al., 2009]. In this study, relapse rates were also decreased from 36% to 13.3% with increasing dose exposure of ribavirin among patients with end-of-treatment response. These results

confirm that maintaining a sufficient dose of ribavirin during the full treatment period could reduce the possibility of relapse, and that an extended duration of therapy for patients with late virological response could increase the chance of achieving sustained virological response, regardless of core aa substitution patterns [Berg et al., 2006; Pearlman et al., 2007; Ferenci et al., 2010].

In this study, the COBAS Amplicor HCV Test v2.0, with a lower limit of detection of 50 IU/ml, was used to assess the serum HCV RNA. Recently, real-time PCR-based HCV RNA assays with a higher sensitivity, COBAS TaqMan HCV assay (Chugai-Roche Diagnostics), with a lower limit of detection of 15 IU/ml, have been introduced. Sarrazin et al. [2010] compared virological response rates that were originally tested by COBAS Amplicor assay with those retested by COBAS TaqMan assay, using the same cohort. Among genotype 1 patients, complete early virological response and sustained virological response rates were similar when virological responses were defined as <50 IU/ml by Amplicor assay (77% and 87%) and <15 IU/ml by TaqMan assay (76% and 88%). Therefore, measuring HCV RNA by the Amplicor assay in this study would have little affects on the results.

In conclusion, the results have demonstrated that substitution of core aa 70 could be independently associated with an insufficient decline in HCV RNA level during first 12 weeks, and substitution of core aa 91 was independently associated with detectable HCV RNA at week 24, all of which were considered to be important negative predictors of attaining sustained virological response in patients with HCV genotype 1 treated with Peg-IFN plus ribavirin. On the other hand, only dose exposure of ribavirin and no complete early virological response was independent predictors of virological relapse among patients with end-of-treatment response, not substitution of core aa 70 or 91. The aa substitution patterns of the HCV core protein can be an important pretreatment predictor for non-response in patients with HCV genotype 1 treated with Peg-IFN plus ribavirin, but not for relapse after the completion of therapy.

REFERENCES

Abe H, Ochi H, Maekawa T, Hayes CN, Tsuge M, Miki D, Mitsui F, Hiraga N, Imamura M, Takahashi S, Ohishi W, Arihiro K, Kubo M, Nakamura Y, Chayama K. 2010. Common variation of IL28 affects gamma-GTP levels and inflammation of the liver in chronically infected hepatitis C virus patients. J Hepatol 53:439–443.

Akuta N, Suzuki F, Sezaki H, Suzuki Y, Hosaka T, Someya T, Kobayashi M, Saitoh S, Watahiki S, Sato J, Matsuda M, Arase Y, Ikeda K, Kumada H. 2005. Association of amino acid substitution pattern in core protein of hepatitis C virus genotype 1b high viral load and non-virological response to interferon-ribavirin combination therapy. Intervirology 48:372–380.

Akuta N, Suzuki F, Kawamura Y, Yatsuji H, Sezaki H, Suzuki Y, Hosaka T, Kobayashi M, Arase Y, Ikeda K, Kumada H. 2007a. Amino acid substitutions in the hepatitis C virus core region are the important predictor of hepatocarcinogenesis. Hepatology 46:1357–1364.

Akuta N, Suzuki F, Kawamura Y, Yatsuji H, Sezaki H, Suzuki Y, Hosaka T, Kobayashi M, Arase Y, Ikeda K, Kumada H. 2007b. Predictive factors of early and sustained responses to peginterferon plus ribavirin combination therapy in Japanese patients infected with hepatitis C virus genotype 1b: Amino acid substitutions in the core region and low-density lipoprotein cholesterol levels. J Hepatol 46:403–410.

Akuta N, Suzuki F, Kawamura Y, Yatsuji H, Sezaki H, Suzuki Y, Hosaka T, Kobayashi M, Arase Y, Ikeda K, Kumada H. 2007c. Predictors of viral kinetics to peginterferon plus ribavirin combination therapy in Japanese patients infected with hepatitis C virus genotype 1b. J Med Virol 79:1686–1695.

Anonymous. 2002. National Institutes of Health Consensus Development Conference Statement: Management of hepatitis C: 2002—June 10–12, 2002. Hepatology 36:S3–S20.

Ariumi Y, Kuroki M, Abe K, Dansako H, Ikeda M, Wakita T, Kato N. 2007. DDX3 DEAD-box RNA helicase is required for hepatitis C virus RNA replication. J Virol 81:13922–13926.

Bedossa P, Poynard T. 1996. An algorithm for the grading of activity in chronic hepatitis C. The METAVIR Cooperative Study Group. Hepatology 24:289–293.

Berg T, von Wagner M, Nasser S, Sarrazin C, Heintges T, Gerlach T, Buggisch P, Goeser T, Rasenack J, Pape GR, Schmidt WE, Kallinowski B, Klinker H, Spengler U, Martus P, Alshuth U, Zeuzem S. 2006. Extended treatment duration for hepatitis C virus type 1: Comparing 48 versus 72 weeks of peginterferon-alfa-2a plus ribavirin. Gastroenterology 130:1086–1097.

Blindenbacher A, Duong FH, Hunziker L, Stutvoet ST, Wang X, Terracciano L, Moradpour D, Blum HE, Alonzi T, Tripodi M, La Monica N, Heim MH. 2003. Expression of hepatitis c virus proteins inhibits interferon alpha signaling in the liver of transgenic mice. Gastroenterology 124:1465–1475.

Bode JG, Ludwig S, Ehrhardt C, Albrecht U, Erhardt A, Schaper F, Heinrich PC, Haussinger D. 2003. IFN-alpha antagonistic activity of HCV core protein involves induction of suppressor of cytokine signaling-3. FASEB J 17:488–490.

Davis GL, Wong JB, McHutchison JG, Manns MP, Harvey J, Albrecht J. 2003. Early virologic response to treatment with peginterferon alfa-2b plus ribavirin in patients with chronic hepatitis C. Hepatology 38:645–652.

de Lucas S, Bartolome J, Carreno V. 2005. Hepatitis C virus core protein down-regulates transcription of interferon-induced antiviral genes. J Infect Dis 191:93–99.

Dienstag JL, McHutchison JG. 2006. American Gastroenterological Association medical position statement on the management of hepatitis C. Gastroenterology 130:225–230.

Donlin MJ, Cannon NA, Yao E, Li J, Wahed A, Taylor MW, Belle SH, Di Bisceglie AM, Aurora R, Tavis JE. 2007. Pretreatment sequence diversity differences in the full-length hepatitis C virus open reading frame correlate with early response to therapy. J Virol 81: 8211–8224.

Ferenci P, Fried MW, Shiffman ML, Smith CI, Marinos G, Goncales FL, Jr., Haussinger D, Diago M, Carosi G, Dhumeaux D, Craxi A, Chaneac M, Reddy KR. 2005. Predicting sustained virological responses in chronic hepatitis C patients treated with peginterferon alfa-2a (40 KD)/ribavirin. J Hepatol 43:425–433.

Ferenci P, Laferl H, Scherzer TM, Maieron A, Hofer H, Stauber R, Gschwantler M, Brunner H, Wenisch C, Bischof M, Strasser M, Datz C, Vogel W, Loschenberger K, Steindl-Munda P. 2010. Peginterferon alfa-2a/ribavirin for 48 or 72 weeks in hepatitis C genotypes 1 and 4 patients with slow virologic response. Gastroenterology 138:503–512 e501.

Fried MW, Shiffman ML, Reddy KR, Smith C, Marinos G, Goncales FL, Jr., Haussinger D, Diago M, Carosi G, Dhumeaux D, Craxi A, Lin A, Hoffman J, Yu J. 2002. Peginterferon alfa-2a plus ribavirin for chronic hepatitis C virus infection. N Engl J Med 347:975–982.

Ge D, Fellay J, Thompson AJ, Simon JS, Shianna KV, Urban TJ, Heinzen EL, Qiu P, Bertelsen AH, Muir AJ, Sulkowski M, McHutchison JG, Goldstein DB. 2009. Genetic variation in IL28B predicts hepatitis C treatment-induced viral clearance. Nature 461: 399–401.

Hadziyannis SJ, Sette H, Jr., Morgan TR, Balan V, Diago M, Marcellin P, Ramadori G, Bodenheimer H, Jr., Bernstein D, Rizzetto M, Zeuzem S, Pockros PJ, Lin A, Ackrill AM. 2004. Peginterferon-alpha2a and ribavirin combination therapy in chronic hepatitis C: A randomized study of treatment duration and ribavirin dose. Ann Intern Med 140:346–355.

Hiramatsu N, Oze T, Yakushijin T, Inoue Y, Igura T, Mochizuki K, Imanaka K, Kaneko A, Oshita M, Hagiwara H, Mita E, Nagase T,

Ito T, Inui Y, Hijioka T, Katayama K, Tamura S, Yoshihara H, Imai Y, Kato M, Yoshida Y, Tatsumi T, Ohkawa K, Kiso S, Kanto T, Kasahara A, Takehara T, Hayashi N. 2009. Ribavirin dose reduction raises relapse rate dose-dependently in genotype 1 patients with hepatitis C responding to pegylated interferon alpha-2b plus ribavirin. J Viral Hepat 16:586–594.

Hu Z, Muroyama R, Kowatari N, Chang J, Omata M, Kato N. 2009. Characteristic mutations in hepatitis C virus core gene related to the occurrence of hepatocellular carcinoma. Cancer Sci 100:2465–2468.

Ikeda F, Dansako H, Nishimura G, Mori K, Kawai Y, Ariumi Y, Miyake Y, Takaki A, Nouso K, Iwasaki Y, Ikeda M, Kato N, Yamamoto K. 2010. Amino acid substitutions of hepatitis C virus core protein are not associated with intracellular antiviral response to interferon-alpha in vitro. Liver Int 30:1324–1331.

Joo M, Hahn YS, Kwon M, Sadikot RT, Blackwell TS, Christman JW. 2005. Hepatitis C virus core protein suppresses NF-kappaB activation and cyclooxygenase-2 expression by direct interaction with IkappaB kinase beta. J Virol 79:7648–7657.

Kato N, Hijikata M, Ootsuyama Y, Nakagawa M, Ohkoshi S, Sugimura T, Shimotohno K. 1990. Molecular cloning of the human hepatitis C virus genome from Japanese patients with non-A, non-B hepatitis. Proc Natl Acad Sci USA 87:9524–9528.

Kobayashi M, Akuta N, Suzuki F, Hosaka T, Sezaki H, Suzuki Y, Arase Y, Ikeda K, Watahiki S, Mineta R, Iwasaki S, Miyakawa Y, Kumada H. 2010. Influence of amino-acid polymorphism in the core protein on progression of liver disease in patients infected with hepatitis C virus genotype 1b. J Med Virol 82:41–48.

Lai MM, Ware CF. 2000. Hepatitis C virus core protein: Possible roles in viral pathogenesis. Curr Top Microbiol Immunol 242:117–134.

Lin W, Kim SS, Yeung E, Kamegaya Y, Blackard JT, Kim KA, Holtzman MJ, Chung RT. 2006. Hepatitis C virus core protein blocks interferon signaling by interaction with the STAT1 SH2 domain. J Virol 80:9226–9235.

Manns MP, McHutchison JG, Gordon SC, Rustgi VK, Shiffman M, Reindollar R, Goodman ZD, Koury K, Ling M, Albrecht JK. 2001. Peginterferon alfa-2b plus ribavirin compared with interferon alfa-2b plus ribavirin for initial treatment of chronic hepatitis C: A randomised trial. Lancet 358:958–965.

McHutchison JG, Manns M, Patel K, Poynard T, Lindsay KL, Trepo C, Dienstag J, Lee WM, Mak C, Garaud JJ, Albrecht JK. 2002. Adherence to combination therapy enhances sustained response in genotype-1-infected patients with chronic hepatitis C. Gastroenterology 123:1061–1069.

McHutchison JG, Lawitz EJ, Shiffman ML, Muir AJ, Galler GW, McCone J, Nyberg LM, Lee WM, Ghalib RH, Schiff ER, Galati JS, Bacon BR, Davis MN, Mukhopadhyay P, Koury K, Noviello S, Pedicone LD, Brass CA, Albrecht JK, Sulkowski MS. 2009. Peginterferon alfa-2b or alfa-2a with ribavirin for treatment of hepatitis C infection. N Engl J Med 361:580–593.

Melen K, Fagerlund R, Nyqvist M, Keskinen P, Julkunen I. 2004. Expression of hepatitis C virus core protein inhibits interferon-induced nuclear import of STATs. J Med Virol 73:536–547.

Nakamoto S, Kanda T, Yonemitsu Y, Arai M, Fujiwara K, Fukai K, Kanai F, Imazeki F, Yokosuka O. 2009. Quantification of hepatitis C amino acid substitutions 70 and 91 in the core coding region by real-time amplification refractory mutation system reverse transcription-polymerase chain reaction. Scand J Gastroenterol 44:872–877.

Okanoue T, Itoh Y, Hashimoto H, Yasui K, Minami M, Takehara T, Tanaka E, Onji M, Toyota J, Chayama K, Yoshioka K, Izumi N, Akuta N, Kumada H. 2009. Predictive values of amino acid sequences of the core and NS5A regions in antiviral therapy for hepatitis C: A Japanese multi-center study. J Gastroenterol 44: 952–963.

Osna NA, White RL, Krutik VM, Wang T, Weinman SA, Donohue TM, Jr. 2008. Proteasome activation by hepatitis C core protein is reversed by ethanol-induced oxidative stress. Gastroenterology 134:2144–2152.

Oze T, Hiramatsu N, Yakushijin T, Kurokawa M, Igura T, Mochizuki K, Imanaka K, Yamada A, Oshita M, Hagiwara H, Mita E, Ito T, Inui Y, Hijioka T, Tamura S, Yoshihara H, Hayashi E, Inoue A, Imai Y, Kato M, Yoshida Y, Tatsumi T, Ohkawa K, Kiso S, Kanto T, Kasahara A, Takehara T, Hayashi N. 2009. Pegylated interferon alpha-2b (Peg-IFN alpha-2b) affects early virologic response dose-dependently in patients with chronic hepatitis C genotype 1 during treatment with Peg-IFN alpha-2b plus ribavirin. J Viral Hepat 16:578–585.

Pearlman BL, Ehleben C, Saifee S. 2007. Treatment extension to 72 weeks of peginterferon and ribavirin in hepatitis c genotype 1-infected slow responders. Hepatology 46:1688–1694.

Romero-Gomez M, Del Mar Viloria M, Andrade RJ, Salmeron J, Diago M, Fernandez-Rodriguez CM, Corpas R, Cruz M, Grande L, Vazquez L, Munoz-De-Rueda P, Lopez-Serrano P, Gila A, Gutierrez ML, Perez C, Ruiz-Extremera A, Suarez E, Castillo J. 2005. Insulin resistance impairs sustained response rate to peginterferon plus ribavirin in chronic hepatitis C patients. Gastroenterology 128: 636–641.

Sarrazin C, Shiffman ML, Hadziyannis SJ, Lin A, Colucci G, Ishida H, Zeuzem S. 2010. Definition of rapid virologic response with a highly sensitive real-time PCR-based HCV RNA assay in peginterferon alfa-2a plus ribavirin response-guided therapy. J Hepatol 52:832–838.

Shirakawa H, Matsumoto A, Joshita S, Komatsu M, Tanaka N, Umemura T, Ichijo T, Yoshizawa K, Kiyosawa K, Tanaka E. 2008. Pretreatment prediction of virological response to peginterferon plus ribavirin therapy in chronic hepatitis C patients using viral and host factors. Hepatology 48:1753–1760.

Strader DB, Wright T, Thomas DL, Seeff LB. 2004. Diagnosis, management, and treatment of hepatitis C. Hepatology 39:1147–1171.

Suppiah V, Moldovan M, Ahlenstiel G, Berg T, Weltman M, Abate ML, Bassendine M, Spengler U, Dore GJ, Powell E, Riordan S, Sheridan D, Smedile A, Fragomeli V, Muller T, Bahlo M, Stewart GJ, Booth DR, George J. 2009. IL28B is associated with response to chronic hepatitis C interferon-alpha and ribavirin therapy. Nat Genet 41:1100–1104.

Tanaka Y, Nishida N, Sugiyama M, Kurosaki M, Matsuura K, Sakamoto N, Nakagawa M, Korenaga M, Hino K, Hige S, Ito Y, Mita E, Tanaka E, Mochida S, Murawaki Y, Honda M, Sakai A, Hiasa Y, Nishiguchi S, Koike A, Sakaida I, Imamura M, Ito K, Yano K, Masaki N, Sugauchi F, Izumi N, Tokunaga K, Mizokami M. 2009. Genome-wide association of IL28B with response to pegylated interferon-alpha and ribavirin therapy for chronic hepatitis C. Nat Genet 41:1105–1109.

Thompson AJ, Muir AJ, Sulkowski MS, Ge D, Fellay J, Shianna KV, Urban T, Afdhal NH, Jacobson IM, Esteban R, Poordad F, Lawitz EJ, McCone J, Shiffman ML, Galler GW, Lee WM, Reindollar R, King JW, Kwo PY, Ghalib RH, Freilich B, Nyberg LM, Zeuzem S, Poynard T, Vock DM, Pieper KS, Patel K, Tillmann HL, Noviello S, Koury K, Pedicone LD, Brass CA, Albrecht JK, Goldstein DB, McHutchison JG. 2010. Interleukin-28B polymorphism improves viral kinetics and is the strongest pretreatment predictor of sustained virologic response in hepatitis C virus-1 patients. Gastroenterology 139:120–129 e118.

Waris G, Felmlee DJ, Negro F, Siddiqui A. 2007. Hepatitis C virus induces proteolytic cleavage of sterol regulatory element binding proteins and stimulates their phosphorylation via oxidative stress. J Virol 81:8122–8130.

Biochemical and Biophysical Research Communications 406 (2011) 614–620

Contents lists available at ScienceDirect

Biochemical and Biophysical Research Communications

journal homepage: www.elsevier.com/locate/ybbrc

Involvement of STAT3-regulated hepatic soluble factors in attenuation of stellate cell activity and liver fibrogenesis in mice

Minoru Shigekawa [a], Tetsuo Takehara [a,*], Takahiro Kodama [a], Hayato Hikita [a], Satoshi Shimizu [a], Wei Li [a], Takuya Miyagi [a], Atsushi Hosui [a], Tomohide Tatsumi [a], Hisashi Ishida [a], Tatsuya Kanto [a], Naoki Hiramatsu [a], Norio Hayashi [b]

[a] *Department of Gastroenterology and Hepatology, Osaka University Graduate School of Medicine, Suita, Osaka, Japan*
[b] *Kansai Rosai Hospital, Amagasaki, Hyogo, Japan*

ARTICLE INFO

Article history:
Received 19 February 2011
Available online 26 February 2011

Keywords:
STAT3
Liver fibrosis
Hepatic stellate cells
Acute phase proteins

ABSTRACT

Glycoprotein 130 (gp130)/signal transducer and activator of transcription 3 (STAT3) signaling in hepatocytes controls a variety of physiological and pathological processes including liver regeneration, apoptosis resistance and metabolism. Recent research has shed light on the importance of acute phase proteins (APPs) regulated by hepatic gp130/STAT3 in host defense through suppression of innate immune responses during systemic inflammation. To examine whether these STAT3-regulated soluble factors directly affect liver fibrogenic responses during liver injury, hepatocyte-specific STAT3 knockout (L-STAT3 KO) mice and control littermates were subjected to bile duct ligation (BDL) and examined 10 days later. In contrast to controls, L-STAT3 KO mice failed to produce APPs, such as serum amyloid A and haptoglobin, after BDL. Whereas L-STAT3 KO mice displayed similar levels of cholestasis, inflammatory cell infiltration and regeneration in the liver, they developed exacerbated liver injury and fibrosis with significant increases in expression of alpha-smooth muscle actin and type I collagen genes. *In vitro* experiments revealed that attenuated expression of APPs in primary hepatocytes isolated from L-STAT3 KO mice with IL-6 exposure, compared to wild-type hepatocytes. The cultured supernatant from IL-6-treated wild-type hepatocytes inhibited expression of alpha-smooth muscle actin and type I collagen genes in activated hepatic stellate cells (HSCs), whereas this did not occur with the supernatant from IL-6-treated knockout hepatocytes or with control medium. In conclusion, the absence of STAT3 in hepatocytes leads to exacerbation of liver fibrosis during cholestasis. Soluble factors released from hepatocytes, dependent on STAT3, collectively play a protective role in liver fibrogenesis through an inhibitory effect on activated HSCs.

1. Introduction

Cholestatic liver injury is characterized by bile flow impairment of different parts of the biliary tree, which can be caused by gallstones, autoimmunity or unknown etiology. Persistent cholestasis eventually progresses toward biliary fibrosis and cirrhosis because of bile acid-induced cholangiocyte and hepatocyte damage, leading to failure of cellular repopulation and excessive deposition of extracellular matrix (ECM) proteins. Hepatic stellate cells (HSCs) are the main ECM-producing cells in the injured liver [1]. Following chronic injury, HSCs activate or transdifferentiate into myofibroblast-like cells, acquiring contractile, proinflammatory and fibrogenic properties. Activated HSCs produce and deposit ECM proteins in the pericentral and periportal regions.

The signal transducer and activator of transcription 3 (STAT3) is known to be ubiquitously expressed in a wide range of tissues where it is activated by tyrosine phosphorylation in response to a variety of cytokines and growth factors (e.g. interleukin (IL)-6 family, IL-10, leptin, IL-17, IL-23, interferons and EGF). STAT3, formerly known as acute phase response factor, regulates the expression of genes involved in the acute phase response, a series of inflammatory reactions induced in response to infection and tissue

Abbreviations: ECM, extracellular matrix; HSCs, hepatic stellate cells; STAT, signal transducer and activator of transcription; IL, interleukin; gp, glycoprotein; APPs, acute phase proteins; L-STAT3 KO, hepatocyte-specific STAT3 knockout; WT, wild-type; BDL, bile duct ligation; TUNEL, terminal deoxynucleotidyl transferase-mediated deoxyuridine triphosphate nick-end labeling; BrdU, 5-bromo-2-deoxyuridine; rtPCR, reverse-transcription polymerase chain reaction; SAA, serum amyloid A; αSMA, alpha-smooth muscle actin; TGFβ, transforming growth factor beta; PDGF, platelet derived growth factor; ALT, alanine aminotransferase.

* Corresponding author. Address: Department of Gastroenterology and Hepatology, Osaka University Graduate School of Medicine, 2-2 Yamada-oka, Suita, Osaka 565-0871, Japan. Fax: +81 6 6879 3629.
E-mail address: takehara@gh.med.osaka-u.ac.jp (T. Takehara).

0006-291X/$ - see front matter © 2011 Elsevier Inc. All rights reserved.
doi:10.1016/j.bbrc.2011.02.105

injury [2]. The IL-6 family is one of the major cytokines involved in triggering the acute phase response and all members of the IL-6 family use glycoprotein 130 (gp130) as a receptor to induce nuclear translocation of STAT3 [3] as well as to activate the Ras/mitogen-activated protein (MAP) pathway. Since systemic deletion of STAT3 leads to embryonic lethality in mice, the significance of STAT3 in adult organs has been investigated using conditional knockout animals generated by the Cre/loxP recombination system [4]. Previous reports suggested that STAT3 signaling in hepatocytes controls a variety of physiological and pathological processes, including hepatocyte proliferation after partial hepatectomy [5], apoptosis resistance of hepatocytes during Fas-mediated liver injury [6] and regulation of hepatic gluconeogenic genes [7]. Further study showed that the soluble factors dependent on gp130/STAT3 signaling such as acute phase proteins (APPs) suppress innate immune cell overactivation and hypercytokinemia, leading to host-defense during systemic inflammation [8,9]. Very recently, research has shown that gp130/STAT3 signaling is protective against liver fibrogenesis by regulating inflammation and injury in the liver during chronic cholestasis [10,11]. However, it is not clear whether STAT3-dependent soluble factors from hepatocyte, such as APPs, affect the activation of HSCs and their collagen synthesis.

In the present study, we used conditional knockout mice, carrying hepatocyte-specific deletion of STAT3, and determined the effects dependent on the hepatocyte-specific STAT3 signaling pathway during cholestasis. We found that its signaling pathway offered protection from liver injury and fibrogenesis in a murine model of cholestatic liver injury. Moreover, STAT3-dependent soluble factors released from hepatocytes directly suppressed the activated HSCs and their collagen synthesis *in vitro*. Hepatocyte STAT3 signaling plays an important role in attenuation of liver disease by modulating liver damage and fibrogenesis through their collective effect on HSCs.

2. Materials and methods

2.1. Animals

Mice carrying a STAT3 gene with 2 loxP sequences flanking exon 22 have been described previously [12]. Hepatocyte-specific STAT3 knockout (L-STAT3 KO) mice were generated by crossing $STAT3^{fl/fl}$ mice with albumin-promoter Cre (Alb-Cre) transgenic mice [13]. Sex-matched $STAT3^{fl/fl}$ mice obtained from the same litter were used as wild-type (WT) controls. All mice were used at the age of 7–10 weeks. All animals were housed with 12-h light/dark cycles with free access to food and water under specific pathogen-free conditions and were treated with humane care under approval from the Animal Care and Use Committee of Osaka University Medical School.

2.2. Bile duct ligation

Bile duct ligation (BDL) is a well-established murine model of cholestasis. L-STAT3 KO mice and WT littermates were subjected to BDL as previously reported [14]. Briefly, the common bile duct was ligated 3 times with 5–0 silk sutures and then cut between the ligatures. After 10 days, the animals were sacrificed for the following analyses.

2.3. Histologic analyses

The liver sections were stained with H&E or picrosirius red. The percentage of oncotic necrosis or fibrotic area was calculated using image analysis software (win-ROOF visual system; Mitani Co., Tokyo, Japan). To assess intrahepatic macrophage accumulation, liver sections were stained with F4/80 using an anti-F4/80 rat monoclonal antibody (Abcam, Cambridge, MA). To detect apoptotic cells, the liver sections were also subjected to terminal deoxynucleotidyl transferase-mediated deoxyuridine triphosphate nick-end labeling (TUNEL) staining as previously reported [15]. To assess regenerative status, nuclear 5-bromo-2-deoxyuridine (BrdU) incorporation was evaluated as previously described [16].

2.4. Isolation and culture of murine hepatic stellate cells

HSCs were isolated from C57BL/6J mice by 2-step collagenase-pronase perfusion of mouse liver as previously described [16]. Activated HSCs after a few passages were cultured with the supernatant from primary hapatocyte or recombinant Apo-SAA (PEPROTECH, Rocky Hill, NJ).

2.5. Primary culture of hepatocytes

Hepatocytes were isolated from the liver of L-STAT3 KO mice and WT mice by 2-step collagenase-pronase perfusion of mouse liver as previously described [8]. Isolated hepatocytes were stimulated with 20 ng/ml recombinant mouse IL-6 (R&D Systems, Minneapolis, MN). The cells or the supernatant were harvested after 24 h.

2.6. Western blot analysis

Western blotting was performed as previously described [16].For immunodetection, the following antibodies were used: phospho-STAT3 (Tyr705) antibody, anti-STAT3 antibody (Cell Signaling Technology, Danvers, MA) and anti-β-actin antibody (Sigma–Aldrich, St. Louis, MO).

2.7. Real-time reverse-transcription polymerase chain reaction

Total RNA extracted from the liver tissue and HSCs were reverse transcribed and subjected to real-time reverse-transcription polymerase chain reaction (rtPCR) as previously described [15]. mRNA expression of the specific genes was quantified using TaqMan Gene Expression Assays (Applied Biosystems Inc., Foster City, CA). Assay IDs of the specific genes are provided in Supplementary Table 1. Transcript levels are presented as fold induction.

2.8. Enzyme-linked immunosorbent assay

The levels of serum amyloid A (SAA) and haptoglobin in serum and cultured supernatant were measured using SAA ELISA kit (Invitrogen, Camarillo, CA) and Mouse Haptoglobin ELISA kit (Immunology Consultants Laboratory, Newberg, OR), according to the manufacturer's protocol.

2.9. Statistical analysis

Data are presented as median and interquartile range or mean ± standard deviation, compared using the Mann–Whitney U test and unpaired *t*-test, respectively. Statistical significance was set at $p < 0.05$.

3. Results

3.1. Lack of acute phase response in L-STAT3 KO mice after BDL

L-STAT3 KO mice were produced by crossing floxed STAT3 mice and Alb-Cre transgenic mice which express Cre recombinase gene under regulation of the albumin gene promoter. To determine the

role of hepatocyte STAT3 during obstructive cholestasis, L-STAT3 KO mice and WT mice were subjected to BDL and examined 10 days later. After BDL treatment, western blot analysis revealed that STAT3 expression in the livers of L-STAT3 KO mice was greatly reduced compared with that of WT mice (Fig. 1A). In contrast to L-STAT3 KO mice, phosphorylation of STAT3 was clearly seen in WT mice with BDL compared with that in sham-operated mice (Fig. 1A). Given that STAT3 is a well-known mediator of APPs in the IL-6/gp130/STAT3 signaling pathway, we analyzed the mRNA expression of APPs such as SAA and haptoglobin by real-time rtPCR. The hepatic expression of SAA and haptoglobin genes was clearly induced after BDL in WT mice (Fig. 1B). In contrast, the hepatic expression of these genes did not increase in L-STAT3 KO mice. We also measured the serum levels of APPs. Similarly, the levels of SAA and haptoglobin clearly increased in WT littermates after BDL and were completely diminished in L-STAT3 KO mice (Fig. 1C).

3.2. L-STAT3 KO mice show progression of liver fibrosis

To examine the effect of hepatocyte-specific STAT3 deficiency on liver fibrosis after BDL, we evaluated hepatic collagen deposition by picrosirius red staining of liver sections (Fig. 2A). Morphometric analysis revealed that collagen deposition increased in both groups after BDL and was more significantly higher in L-STAT3 KO mice than in the WT littermates (Fig. 2B). As type I collagen is known to be a major form of collagen in cirrhosis, we analyzed hepatic expression of type I collagen α1 gene, *col1a1*. The levels more significantly increased in L-STAT3 KO mice than WT mice (Fig. 2C). HSCs are main collagen-producing cells in the injured liver and alpha-smooth muscle actin (αSMA) is the marker of activation of HSCs. The expression levels of αSMA gene, *acta2*, were significantly higher in L-STAT3 KO mice than WT controls after BDL (Fig. 2C). The mRNA expression of both transforming growth factor beta (TGFβ), as an important profibrogenic cytokine, and platelet derived growth factor (PDGF), which is the most potent mitogen for HSCs, were not significantly different between the two groups after BDL (Fig. 2D).

3.3. L-STAT3 KO mice display exacerbated liver injury

We examined liver injury and cholestasis upon BDL. There was no significant difference in cholestasis between the two groups after BDL as evidenced by serum levels of total bilirubin and alkaline phosphatase, but L-STAT3 KO mice showed increased levels of serum alanine aminotransferase (ALT) compared with WT controls (Fig. 3A). Oncotic necrosis, known as bile infarcts, is a characteristic feature of liver injury in the BDL model. The area of oncotic necrosis in the liver was not significantly different between the two groups after BDL (Fig. 3B). TUNEL staining of the liver sections revealed that the numbers of apoptotic cells in the liver more significantly increased in L-STAT3 KO mice than in WT littermates after BDL (Fig. 3C). We examined liver regeneration by BrdU incorporation in liver sections (Supplementary Fig. 1A). There was no significant difference between the two groups as determined by the count of BrdU-positive cells after BDL (Fig. 3D). Kupffer cells are resident macrophages that play a major role in liver inflammation by releasing cytokines. The F4/80 antigen is expressed on a wide range of mature tissue macrophages including Kupffer cells, and we thus examined F4/80 staining of liver sections (Supplementary Fig. 1B). There was no significant difference in the count of F4/80-positive cells between the two groups after BDL (Fig. 3E). The hepatic mRNA expression of CD68, expressed on monocytes/macrophages, CD4 and CD8, both of which are surface markers of T cells, was not significantly different between the two groups after BDL (Fig. 3F, Supplementary Fig. 2).

3.4. Soluble factors released from IL-6-treated hepatocytes are involved in suppression of activated HSCs and inhibition of their collagen production

In our *in vivo* study, we revealed the exacerbation of cholestasis-induced liver fibrosis and the increases in hepatic expression of αSMA and type I collagen α1 genes in L-STAT3 KO mice. Furthermore, the acute phase response induced after BDL was invisible in L-STAT3 KO mice. We hypothesized that STAT3-mediated soluble

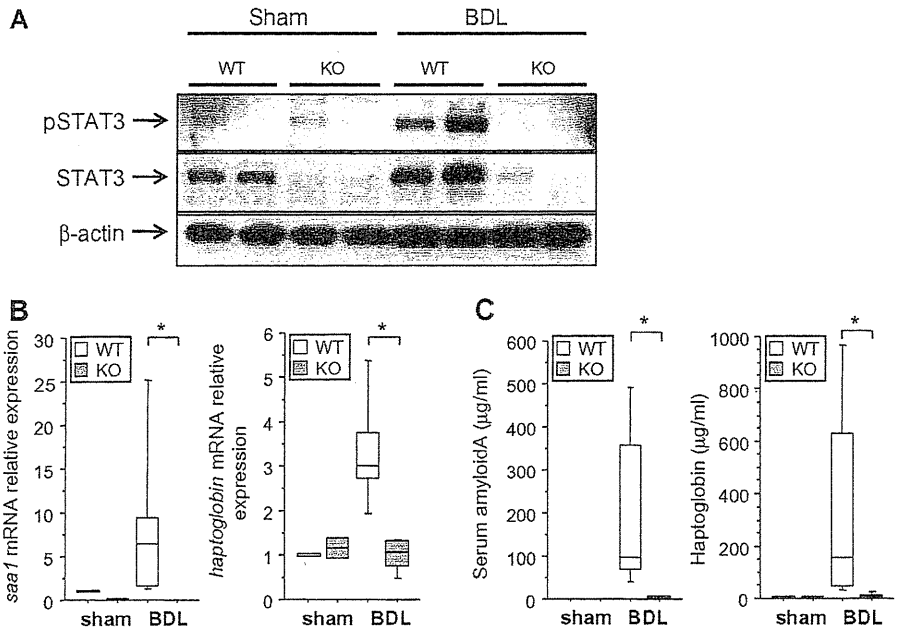

Fig. 1. Activation of STAT3 and production of acute phase proteins in the liver after BDL. L-STAT3 KO mice (KO) and WT littermates (WT) were subjected to BDL or sham-operation (sham) and examined 10 days later. (A) Expressions of STAT3 and phosphorylated STAT3 (pSTAT3) in the liver were assessed by western blot analysis. β-actin is included as a control. (B) Hepatic mRNA expression of SAA and haptoglobin was determined by real-time rtPCR analysis, $n = 8$/group, $^*p < 0.05$. (C) Serum levels of SAA and haptoglobin were determined by ELISA, $n = 8$/group, $^*p < 0.05$.

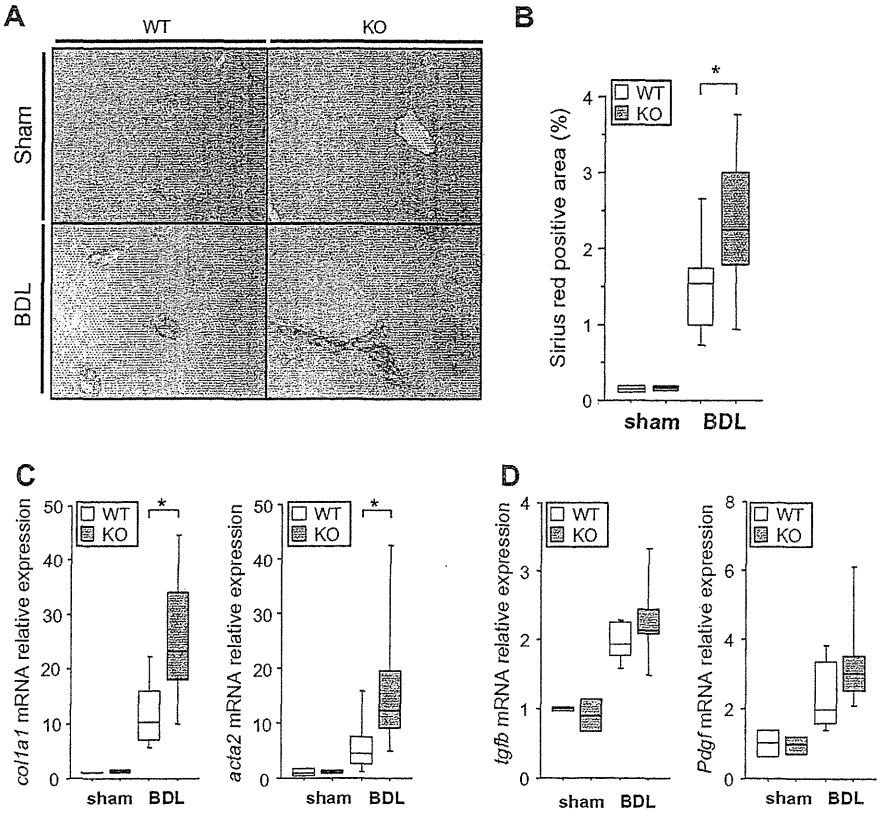

Fig. 2. Exacerbation of liver fibrosis in L-STAT3 KO mice after BDL. L-STAT3 KO mice (KO) and WT littermates (WT) were subjected to BDL or sham-operation (sham) and examined 10 days later. (A) Representative views of picrosirius red staining of the liver sections. (B) Morphometric analysis for picrosirius red staining, $n = 8$/group, $^*p < 0.05$. (C) Hepatic expression of αSMA and type I collagen α1 genes by real-time rtPCR analysis, $n = 8$/group, $^*p < 0.05$. (D) Hepatic expression of TGFβ and PDGF genes by real-time rtPCR analysis, $n = 8$/group.

factors released from hepatocytes repressed activated HSCs and their collagen synthesis. We isolated primary hepatocytes from L-STAT3 KO mice and WT controls, and stimulated them with or without IL-6. The cultured medium of stimulated hepatocytes was collected after 24 h. Whereas faint signals of STAT3 phosphorylation were observed under resting conditions in WT hepatocytes, administration of IL-6 clearly activated STAT3 phosphorylation in WT hepatocytes in contrast to STAT3 KO hepatocytes (Fig. 4A). Accordingly, IL-6 administration activated SAA and haptoglobin gene expression in WT hepatocytes, leading to production of higher levels of SAA and haptoglobin in culture supernatant compared with STAT3 KO hepatocytes (Fig. 4B, Supplementary Fig. 3).

Activated HSCs isolated from C57BL/6J were cultured with supernatant taken from IL-6-treated WT hepatocytes (sup-WT) or that from IL-6-treated STAT3 KO hepatocytes (sup-KO). Activated HSCs were also incubated with medium containing the same amount of IL-6 (sup-control) as a control. The mRNA expression of αSMA and type I collagen α1 in HSCs cultured with sup-WT significantly decreased compared with sup-control (Fig. 4C). On the other hand, the expression of these genes in HSCs cultured with sup-KO was similar to the levels of sup-control (Fig. 4C). In addition, activated HSCs were cultured with recombinant SAA. The expression of αSMA gene in HSCs decreased in dose-dependent manner, although the expression of type I collagen α1 gene did not change (Fig. 4D).

4. Discussion

Liver fibrosis is a consequence of chronic liver injury and inflammation. Accumulating evidence suggests that liver fibrosis is to some extent reversible by appropriate therapeutic intervention for chronic liver diseases [1]. Clarifying the cellular and molecular mechanisms involved in fibrogenesis and its progression has become very important for efficacious treatment. In the present study, we used L-STAT3 KO mice to examine the significance of this signaling pathway in liver fibrogenesis, because hepatocyte STAT3 is a crucial signaling transducer and transcription factor that regulates most, if not all, APPs which have been shown to possess a variety of biological properties during inflammation. We have demonstrated here that lack of STAT3 accelerates liver fibrosis during cholestasis and suggested that STAT3-dependent soluble factors collectively serve as a negative regulator for activation of HSCs.

Very recent research has shown that lack of gp130 or STAT3 in hepatocytes exacerbates liver fibrosis in murine sclerosis cholangitis models induced by 3,5-diethoxycarbonyl-1,4-dihydrocollidine (DDC) diet or genetic deletion of multidrug resistance gene 2 (*mdr2*), respectively. In those studies, deletion of gp130 or STAT3 induced severer cholestasis compared with control mice, leading to enhanced inflammatory cell infiltration and injury in the liver [10,11]. Therefore, exacerbation of liver fibrosis observed in those models might be ascribed to exacerbated cholestasis and liver